



Cite this: *Mater. Adv.*, 2022, 3, 3709

## Research progress on nano-sensitizers for enhancing the effects of radiotherapy

Yuan Zhang,<sup>†,a</sup> Xiao Han,<sup>†,a</sup> Yuan Liu,<sup>a</sup> Shuang Wang,<sup>a</sup> Xianlin Han<sup>\*b</sup> and Cui Cheng<sup>ID, \*a</sup>

Radiotherapy (RT) is local control of tumors using radiation, including external irradiation (EBRT) and internal irradiation (RIT). Cancer radiotherapy based on external beams is a major clinical treatment for cancer, which has been widely used in the treatment of more than one-third of local solid tumors. However, due to the tumor's insensitivity to radiation, low absorption rate of radiation by tumors, large radiation doses are often needed during radiotherapy, causing serious damage to normal tissues near the tumors. The most important is that the extent of cancer cell damage caused by radiotherapy and the radiosensitivity of tumors is mainly determined by the concentration of oxygen. The above two aspects severely limit the effect of radiotherapy. Nano-sensitizers can effectively accumulate radiation doses and enhance radiation effects, thereby improving the efficacy of radiotherapy. In addition, nano-sensitizers can also increase tumor sensitivity to radiation through reactive oxygen species (ROS). Therefore, this article reviews the latest progress of nano-sensitizers for radiotherapy, which is focused on precious metal-based nano-sensitizers, rare earth metal-based nano-sensitizers, semiconductor metal-based nano-sensitizers, other metal- and nonmetal-based nano-sensitizers. And the recent literature reports and applications of the nano-sensitizers are also discussed.

Received 28th January 2022,  
Accepted 20th March 2022

DOI: 10.1039/d2ma00094f

rsc.li/materials-advances

## 1. Introduction

According to data from the World Health Organization (WHO), the number of cancer-related deaths each year is expected to increase by 45% from 2007 to 2030.<sup>1</sup> About 17.5 million new cancer cases were reported worldwide, with 8.7 million cancer-related deaths in 2015.<sup>2</sup> Sadly, it is estimated that the number of new cancer cases reached 19.3 million globally, and nearly 10 million people died from cancer in 2020, according to the updated estimates of cancer incidence and mortality at the end of 2020 from the GLOBOCAN 2020.<sup>3</sup> Cancer is still the main cause of death for people in most countries in the world.

Radiation therapy (RT) is one of the mainstream tumor treatments alongside chemotherapy and surgery.<sup>4,5</sup> In the current clinical cancer treatment, about half of the cancer patients will use radiotherapy or combine it with other treatment methods in the process of cancer treatment.<sup>6</sup> Radiotherapy is a key method in the treatment of malignant tumors, and its role and status are becoming increasingly prominent. The treatment principle of RT is that high-energy

ionizing radiation (such as  $\gamma$ -rays and X-rays) directly interacts with the cell DNA, causing DNA damage (DNA is the main target that determines radiobiological effects),<sup>7</sup> or indirectly reacts with water molecules to produce ROS to damage DNA or other cellular components, inducing apoptosis and necrosis.<sup>8</sup> Radiotherapy mainly includes internal radioisotope therapy (RIT) and external radiation therapy (EBRT). RIT uses a minimally invasive method to introduce therapeutic radioisotopes into tumors to induce cancer cell death. EBRT uses high-energy X-beams, electron beams, or proton beams from outside the body to directly irradiate tumors.<sup>9</sup>

Although the role of radiotherapy has become increasingly prominent, its therapeutic effect is not ideal. The hypoxia problem in most solid tumors hinders the effect of radiotherapy to a large extent, and oxygen is critical to increase radiation-induced DNA damage.<sup>10</sup> In the 1930s, Crabtree and Cramer<sup>11</sup> showed that molecular oxygen is a key determinant of the cell's response to radiation. In addition, since the therapeutic effect of radiotherapy depends on the patients' radiosensitivity, its complete cure rate is very low.<sup>12</sup> In order to effectively destroy cancer cells and inhibit tumor growth, large doses of X-rays are usually required, especially when treating deep-seated tumors; however, the radiation resistance caused by the tumor's hypoxic environment cannot be alleviated by high-dose radiotherapy, and it can also severely damage normal tissues and cause toxic side effects.<sup>13</sup> Therefore, it is necessary

<sup>a</sup>College of Biological Science and Engineering, Fuzhou University, Fuzhou 350108, China. E-mail: ibptcc@fzu.edu.cn

<sup>b</sup>Department of General Surgery, Peking Union Medical College Hospital, Beijing, 100730, P. R. China. E-mail: hanxianlin@pumch.cn

† Yuan Zhang and Xiao Han contributed equally to this work.



to seek a high-efficiency, low-toxicity radiosensitizer to improve the tumors' radiosensitivity and reduce the damage to the surrounding normal cells.

In the past ten years, the rapid development of emerging advanced nanomaterials, nanobiotechnology and nanomedicine has provided a good opportunity for tumor radiosensitization,<sup>6</sup> because nanomaterials have the following excellent physical and chemical properties: good biocompatibility, inherent radiosensitization activity, high loading of multiple drugs, enhanced tumor tissue permeability and retention (EPR) effects, *etc.* Nanomaterials have been widely studied and applied in improving the effect of radiotherapy.<sup>14</sup> In recent years, new nano-radiosensitizers and methods of radiosensitization have been continuously proposed.<sup>15</sup> The types of nanomaterials are not limited to precious metals (silver (Ag), gold (Au), and platinum (Pt)); some nanomaterials that are based on rare earth metals (gadolinium (Gd), hafnium (Hf), *etc.*), semiconductor metals (bismuth (Bi)), and other metals (titanium (Ti), *etc.*) and non-metal radiosensitizers are also widely used. The classification of main element-based nanomaterials as radiosensitizers is shown in Fig. 1. Therefore, this article systematically summarizes the classification and research results of nano-radiosensitizers as it is very necessary to make a new summary of the latest developments in this field. On the basis of studying its existing research results, it is more important to promote further research and development in this field.

## 2. Precious metal-based nano-radiosensitizers

In the past, precious metal-based nano-radiosensitizers have been the most researched. Due to the strong X-ray attenuation ability of precious metal elements, they can accumulate the radiation dose on cancer cells, thereby achieving the effect of radiotherapy sensitization.<sup>16</sup> The multiple advantages of two precious metals Au and Ag make them superior to other

materials in the preparation of nanomaterials, including low toxicity, easy preparation, easy surface functionalization, high chemical stability, good biocompatibility, controllable size and morphology.<sup>17</sup>

The underlying mechanism of the radiation sensitization of gold-based nanostructures is as follows: due to the high X-ray absorption coefficient of gold nanoparticles (GNPs), secondary electrons (such as Compton electrons, photoelectrons, Auger electrons) and fluorescent photons are emitted under X-ray irradiation, which will lead to ionization of water molecules or intracellular components and increase the local radiation dose.<sup>18</sup> In addition, GNPs have attracted the interest of researchers due to their low toxicity, easy to achieve surface modification and wide photoelectric cross section. Ma *et al.*<sup>18</sup> prepared gold nanospikes (GNSs) with different surface functionalizations (TAT-GNSs NH<sub>2</sub>-GNSs, FA-GNSs) and evaluated their radiation sensitization effects. *In vitro* studies have demonstrated that the ionizing radiation effects of these GNSs have a good correlation with their cell uptake, and the ratio of the sensitization enhancement (SER) of TAT-GNSs reaches 2.30 at a radiation dose of 4 Gy, showing a significant radiation sensitization effect. Ma *et al.*<sup>19</sup> also synthesized GNSs, GNPs and gold nanorods (GNRs) with different shapes but closed average particle diameters (~50 nm), and modified them with nano-polyethylene glycol (PEG) molecules. The cell uptake ability increased in the order of GNPs > GNSs > GNRs, and their SER values were 1.62, 1.37, and 1.21, respectively, indicating that the shape of gold-based nanomaterials also had a very important effect on tumor radiotherapy. It is noteworthy that previous studies have assumed that spherical cells are located in the central nucleus. However, tumor cells are usually not spherical, but have complex shapes. Then, Sung *et al.*<sup>20</sup> evaluated the biological effects of GNPs on cells with different geometric shapes. Human breast cancer cells and rat glioma cells were used as models, when the nucleus was close to the cell membrane, the SER value increased to 1.2 times. Furthermore, the interaction between GNPs and low-energy photons at the nanoscale was simulated using a microcomputer, and the results were applied to biological models to quantify the dependence of GNP radiosensitization on cell geometry. The dose was less than 1% of the surface dose at a distance of about 100 nm from GNPs, indicating that the shape, size and other geometric parameters and position of cells and nuclei were very important for evaluating GNP-mediated radiosensitization. It also proved that the use of low energy photons could effectively enhance the feasibility of radiosensitization therapy for GNP-mediated superficial tumors such as breast cancer and glioma close to the skull. Particularly, for glioma and glioblastoma, GNPs could be injected directly at the surgical site, which dramatically reduces the complications associated with GNP transmission across the BBB to the target. This is the first time that the dependence of GNP radiosensitization on cell geometry was testified. Jia *et al.*<sup>21</sup> synthesized atomic precision gold nanoclusters (Au<sub>8</sub>NCs) with a diameter of about 2 nm, as showed in Fig. 2a. When X-ray irradiated Au<sub>8</sub>NCs, they produced ROS, leading to irreversible apoptosis (Fig. 2b). X-ray

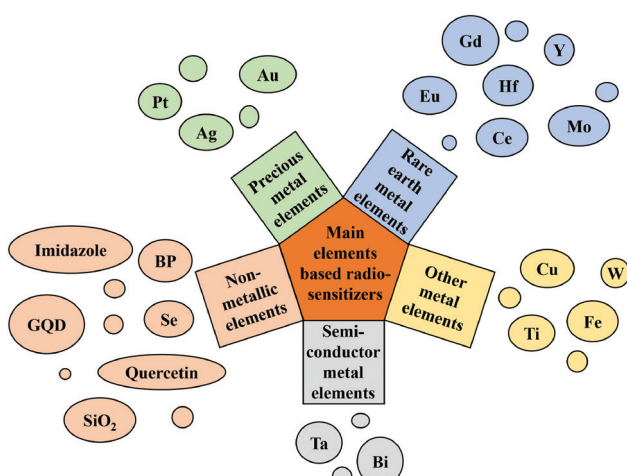


Fig. 1 Classification of main element-based nanomaterials as radiosensitizers.



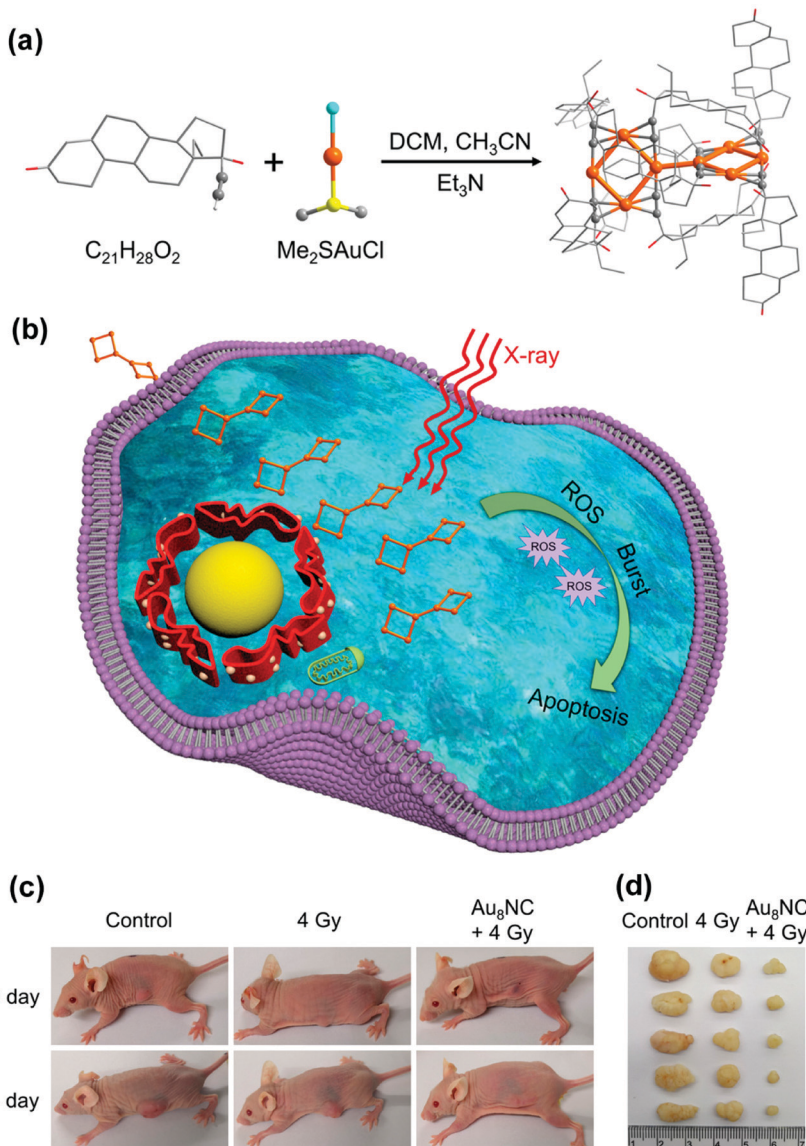


Fig. 2 (a) Synthetic schematic of  $\text{Au}_8\text{NCs}$ ; (b)  $\text{Au}_8\text{NCs}$  for cancer radiotherapy via the ROS burst; (c) representative images of mice treated under various conditions at days 0 and 14; (d) images of dissected tumors. Copyright © 2019 American Chemical Society. Reprinted from ref. 21 with permission.

irradiation (4 Gy) in conjunction with  $\text{Au}_8\text{NCs}$  reduced the cell survival rate to 2.7% and showed a tumor inhibition rate of 74.2% (Fig. 2c and d). The nano-radiosensitizer established in this study not only reduced the X-ray doses, but also reduced the side effects of radiation on normal tissues. As an atomically accurate radiosensitizer, the success of  $\text{Au}_8\text{NCs}$  provided a prospect for the design of a radiosensitizer at the atomic level. Similarly, Kamkaew *et al.*<sup>22</sup> designed polyethylene glycol (PEG) functionalized nanoparticles (Au-Pt NPs) which were composed of metallic elements Au and Pt. Au-Pt nanoparticles had anti-enzyme activity, could catalyze the conversion of  $\text{H}_2\text{O}_2$  to  $\text{O}_2$ , and had the synergistic radiosensitization effect in tumor treatment, which could enhance the deposition of X-ray energy. Compared with the control group, Au-Pt nanoparticles could significantly inhibit tumor growth by reducing tumor hypoxia under X-ray irradiation. Yang *et al.*<sup>23</sup> also prepared polyethylene

glycol (PEG) functionalized nanoparticles composed of metallic elements Au and Pt to improve their co-radiosensitivity. Liu *et al.*<sup>24</sup> prepared pegylated  $\text{Au}@\text{Pt}$  nanodendrites. The shape of nanoparticles was different from that mentioned in the previous studies of Yang *et al.*<sup>23</sup> and Liu *et al.*,<sup>24</sup> but they still had good radiation sensitization. Shi *et al.*<sup>25</sup> enhanced radiotherapy of HCT116 human colon cancer cells by tiopronin-coated GNPs (Tio-GNPs) in combination with low-energy X-ray, and found that intratumoral injection of nanoparticles resulted in 94 times more radiation accumulation than intravenous injection, suggesting that GNPs are indeed an effective radiosensitizer. Bhattacharai *et al.*<sup>26</sup> evaluated the effects of pegylated gold nano-triangles (PAuNTs) on uptake, cytotoxicity, biodistribution and radiosensitization of human glioblastoma multiforme (GBM) cells. Despite extensive literature on the effectiveness of metal nanoparticles as radiosensitizers, much remains unknown



regarding the definition of the ideal shape, size, therapeutic cell type and shape of nanoparticles to improve the efficacy of radiotherapy.

Silver nanoparticles (AgNPs) have also attracted great attention due to their common and excellent radiation sensitization.<sup>27</sup> Xu *et al.*<sup>28</sup> reported that AgNPs had a radiosensitization effect on glioma cells. AgNPs of different particle sizes (20 nm, 50 nm and 100 nm) had different sensitization effects to radiation. The radiosensitization effect of AgNPs reduced with the increasing particle size. Subsequently, Swanner *et al.*<sup>29</sup> demonstrated that AgNPs exhibited radiosensitization in breast cancer tumor cells. And then, more researchers experimentally proved that AgNPs have therapeutic effects on other tumor cells, such as liver cancer, lung cancer and leukemia.<sup>30–32</sup> As a novel nano-radiosensitizer, AgNPs have shown good radiosensitization performance in radiotherapy, but their ability to efficiently enter and accumulate in tumor cells remains to be improved. Hence, targeted modification of AgNPs was aimed to solve this problem. Habiba *et al.*<sup>33</sup> synthesized PAgNPs by modifying AgNPs with pegylated graphene quantum dots (GQDs), which showed good intracellular uptake and radiation sensitization in radiation-resistant HT29 colorectal cancer cells. At 10 Gy of X-ray radiation, nanoparticles have significantly reduced the growth of tumors and prolonged survival compared to radiotherapy alone. Similarly, Zhao *et al.*<sup>34</sup> synthesized AgNPs modified with polyethylene glycol (PEG) and aptamer AS1411 (AsNPs). AsNPs have been shown to specifically target C6 glioma cells without entering normal human microvascular endothelial cells. Results also showed that AsNPs had better radiation sensitization than AgNPs and PEGylated AgNPs (PNPs) and induced a higher apoptosis rate. Meanwhile, Zhao *et al.*<sup>35</sup> also designed AgNPs coated with AS1411, verapamil (VRP) and bovine serum albumin (BSA) (AgNPs@BSA-AS-VRP). The results showed that the mixture of AgNPs@BSA-AS and AgNPs@BSA-AS-VRP (19:1) could significantly accumulate in tumor cells, and the corresponding SER value was 1.55, which significantly improved the therapeutic effect of radiotherapy. As a highly effective nanometer radiosensitizer, it had great potential in the radiotherapy of glioma. Similarly, Liu *et al.*<sup>36</sup> confirmed that the *in vivo* 50% inhibitory concentration (IC50) values of AgNPs on hypoxic U251 cells and C6 cells were 30.32  $\mu\text{g mL}^{-1}$  and 27.53  $\mu\text{g mL}^{-1}$ , respectively. SER indicated that the radiosensitization of AgNPs to hypoxia cells was significantly increased than that of normoxic cells.

Although GNPs and AgNPs have excellent radiosensitization, which one has better radiosensitization effects has aroused intense attention. Liu *et al.*<sup>37</sup> have assessed and compared the effect of GNPs and AgNPs on glioma *in vitro* and *in vivo*. The results confirmed that AgNPs had a stronger radiosensitization ability than GNPs at the same mass and molar concentration, which causes a higher apoptosis rate. In addition, AgNPs + radiation significantly increased autophagy levels compared with GNPs + radiation. In conclusion, the sensitization effect of gold nanoparticles depends on the shape and size of nanoparticles, the type of the surface modifier and the shape of tumor cells. However, AgNPs are not as inert as GNPs; their

biological mechanism of radiation sensitization and synergistic effect may be more complex.<sup>38</sup>

### 3. Rare earth metal-based nano-radiosensitizers

Rare earth elements with high Z values (57–71) are significant to improve the application of radiotherapy.<sup>39</sup>

Gd is a lanthanide element commonly used as a positive contrast agent for magnetic resonance imaging (MRI),<sup>40</sup> and Gd-based nanoparticles (GdNPs) are also attractive due to their radiation-enhancing properties.<sup>41,42</sup> Gd as a promising radiosensitizer could be used in radiosensitizing therapy because of its high X-ray photon capture cross-section and Compton scattering effect.<sup>43</sup> Li *et al.*<sup>44</sup> prepared gadolinium oxide nanocrystalline (GON) and found that the SER at 10% survival level was correlated with the concentration of Gd in NSCLC cells, the maximum SER values of GONs at 10% cell survival fraction (SF<sub>10</sub>) were 1.10, 1.11, and 1.20 for A549, NH1299 and NH1650 cells under carbon ion irradiation. Wu *et al.*<sup>45</sup> designed hyaluronic acid (HA) modified Gd<sub>2</sub>O<sub>3</sub> nanoparticles with targeting and radiosensitization functions to overcome inherent radioresistance and inaccurate tumor localization. Similarly, Andoh *et al.*<sup>46</sup> used gadolinium-loaded chitosan nanoparticles (Gd-Nano CPs) to treat melanoma cells. Zangeneh *et al.*<sup>47</sup> doped Gd into ZnO nanoparticles to prepare Gd-doped ZnO NPs, in which Gd acted as a radiosensitizer. SER values of 10 and 20  $\mu\text{g mL}^{-1}$  nanoparticles were 1.47 and 1.61 under 6 mV X-ray radiation, which exhibited a dose-dependent manner. Huang *et al.*<sup>48</sup> constructed a kind of nanoparticle coordination polymer (H@Gd-NCPs) based on Gd-heme chloride to perform X-ray deposition and glutathione depletion simultaneously. As shown in Fig. 3, H@Gd-NCPs could effectively enhance X-ray absorption and produce more ROS, especially hydroxyl radical within tumor tissues. Hemin encapsulated in H@Gd-NCPs could enhance peroxidase-like properties to utilize overexpressed H<sub>2</sub>O<sub>2</sub> in the tumor microenvironment to deplete GSH. The integration of ROS enhancement and GSH depletion eventually amplified irradiation mediated oxidative stress and induced ICD. Sun *et al.*<sup>49</sup> designed Gd-rose bengal coordination polymer nanodots (GRDs), which have better X-ray absorption than bengal roses alone. Both Lee *et al.*<sup>50</sup> and Ma *et al.*<sup>51</sup> synthesized Gd@C-dots using different methods and achieved a good radiosensitization effect. Most importantly, Dufort *et al.*<sup>52</sup> prepared Gd nanoparticles (AGuIX NPs) with ultra-small particle sizes ( $3.0 \pm 1.0$  nm) for radiosensitization. Du *et al.*<sup>53</sup> studied the sensitization and therapeutic effect of AGuIX NPs in radiotherapy of H1299 non-small cell lung cancer cells. It showed that AGuIX NPs exhibit a high absorption of the photons emitted by the radiation beam, which enhanced the local dose deposition. In a further study, Verry *et al.*<sup>54</sup> prepared AGuIX NPs containing a polysiloxane nucleus surrounded by a ring ligand of Gd. The *in vitro* experiments showed that the addition of AGuIX (from 0.1 mm to 1.0 mm) increased the radiation efficiency by 1.1~2.5 times, and the sensitization



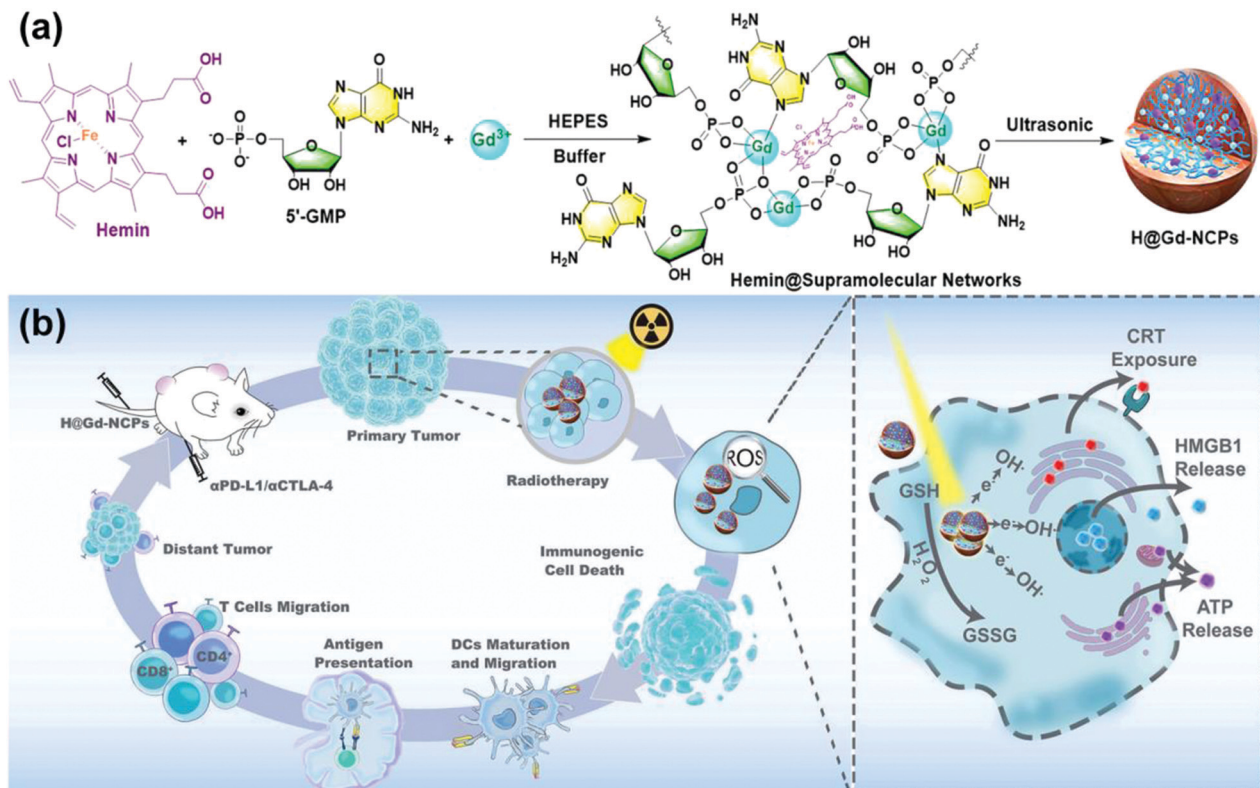


Fig. 3 (a) Synthetic schematic of H@Gd-NCPs; (b) The mechanism of H@Gd-NCPs for radiosensitization via amplifying intracellular oxidative stress to potentiate checkpoint blockade immunotherapies. Copyright © The Author(s) 2021. Reprinted from ref. 48 with permission.

effect was depended on the cell line and the photon beam energy (6 mV~50 kV). AGuIX was also demonstrated as a radiosensitizer in 6 animal tumor models. In a rat model of intracranial glioma, the overall survival rate of the AGuIX injection group was 2 times higher than that of radiotherapy alone. AGuIX combined with WBRT significantly improved survival by 25% in mouse models of multiple melanoma brain metastases (B16F10). In a pancreatic tumor model (CAPAN-1), sensitization therapy significantly reduced tumor growth by 50% compared with radiation alone. AGuIX had good toxicity in rats and even non-human primates, could be directly administered, intravenously and possessed imaging and radiosensitization properties, which prompted its use in patients. This is also the first time that it has been injected into humans. Meanwhile, AGuIX was also reported to have sensitization therapy effects to squamous cell carcinoma of head and neck SQ20B,<sup>55</sup> glioblastoma U-87 MG,<sup>56</sup> cervical cancer HeLa,<sup>57</sup> pancreatic cancer CAPAN-118<sup>58</sup> and melanoma B16F10.<sup>59</sup> Afterwards, Lux *et al.*<sup>60</sup> summarized preclinical evidence supporting AGuIX's transfer to the first human clinical evaluation. Sancey *et al.*<sup>61</sup> translated AGuIX into a phase I clinical evaluation for the treatment of brain metastases and advanced cervical cancer.

Hf metal, a rare earth metal, has often been used in the X-ray manufacturing industry because of its ability of electron emission. It is a material which plays a crucial role in the atomic energy industry and has also been used in medical research and

use.<sup>62</sup> Hf-based nanomaterials have strong X-ray attenuation capabilities, and are widely studied not only for their physical effects, but also for their chemical and biological effects (negligible toxicity and chemical inertia).<sup>63</sup> Hf element could not only enhance the effect of RT by absorbing X-ray energy, but also transform  $\text{H}_2\text{O}$  and  $\text{O}_2$  into some ROS and induce cell apoptosis. Chen *et al.*<sup>64</sup> designed enzyme-like, folic acid modified, Hf-based manganoporphyrin metal-organic framework nanoparticles (MnTCPP-Hf-FA MOF NPs) for targeted tumor radiotherapy and overcoming radiation resistance induced by hypoxia. Hf could absorb X-ray energy, transform  $\text{H}_2\text{O}$  and  $\text{O}_2$  into some ROS and induce cell apoptosis. Hence, the nanoparticles could effectively inhibit the growth of melanoma and prevent tumor recurrence after a single X-ray irradiation with intravenous injection. Gong *et al.*<sup>65</sup> constructed Hf-nMOFs functioned by  $\text{Fe}^{3+}$  (Hf-BPY-Fe). Under radiographic radiation,  $\text{Hf}^{4+}$  produced a huge number of high-energy electrons, some of which converted  $\text{H}_2\text{O}$  to  $\cdot\text{OH}$ , positioning the cell cycle in the radiation-sensitive  $\text{G}_2/\text{M}$  phase and down-regulating DNA repair related proteins to reduce DNA self-repair. The calculated sensitization enhancement ratios by using the model of multi-target single-hit for Hf-BPY and Hf-BPY-Fe were 1.41 and 1.74, which almost achieved ideal radiotherapy results. Liu *et al.*<sup>66</sup> prepared coordination polymer nanoparticles with strong RT and RDT effects by using aggregation induced luminescent materials (AIE) and Hf nanoparticles. Hf could not only absorb X-rays as a nano-radiosensitizer to

enhance RT storage of radiation energy, but also acted as an intermediary to transfer X-ray energy for RDT. Hf-AIE-PEG significantly enhanced tumor growth inhibition compared to RT/PDT alone in the control group. Results also showed that Hf-AIE-PEG-DBCO could generate effective  $\cdot$ OH and radiosensitization under X-ray irradiation, realizing most anticancer efficiency by synchronous RDT and RT.

As a member of the most abundant rare natural element in the earth's crust, cerium (Ce) is also a high Z metal which has been widely used in the medical field. Zhong *et al.*<sup>67</sup> firstly reported the cerium (Ce)-doped NaCeF<sub>4</sub>:Gd, Tb scintillating nanoparticles (SCNPs), which had good radiosensitization through the photoelectric effect and synchronous RT/RDT could be achieved to significantly inhibit tumor growth. Sun *et al.*<sup>68</sup> constructed cisplatin loaded LiLuF<sub>4</sub>:Ce<sup>3+</sup> scintillation nanoparticles (NPs + Cis) to enhance tumor radiosensitivity. Besides, the newly synthesized Ce oxide nanoparticles (CONPs) were also studied. The researchers have investigated the inherent toxicity of CONPs to cancer cells of various origins, including alveolar epithelial cancer cells,<sup>69</sup> hepatocellular carcinoma cells<sup>70</sup> and pancreatic carcinoma cells.<sup>71</sup> Goushbolagh *et al.*<sup>72</sup> studied the radiation dose reduction factors (DRFs) of CONPs in MRC-5 human lung fibroblasts and MCF-7 breast cancer cells. Wason *et al.*<sup>73</sup> demonstrated the production of ROS in CONP treated cancer cells for RT. The mechanism of CONPs in specifically killing cancer cells was that ROS drove the oxidation of thioredoxin 1 (TRX1) and activated c-Jun terminal kinase (JNK), resulting in the activation of apoptosis signaling kinase 1 (ASK1) to induce apoptosis. After this, Ce oxide based nanoparticles were supported as a novel tumor tissue sensitizer. Jiang *et al.*<sup>74</sup> prepared a kind of spindle-shaped CuS@CeO<sub>2</sub> NPs made up of mixed Ce elements (Ce(IV) and Ce(III)) and CuS NPs. CeO<sub>2</sub> could function as a nanoenzyme to catalyze endogenous H<sub>2</sub>O<sub>2</sub> in the tumor tissue into O<sub>2</sub>, which remodeled the hypoxic microenvironment into the one susceptible to RT. At the same time, it could also combine self-supplied oxygen, photothermal capacity and RT sensitivity for cancer treatment. Zhou *et al.*<sup>75</sup> fixed CeO<sub>2</sub> nanoparticles with two-dimensional graphite acetylene (GDY) to form a GDY-CeO<sub>2</sub> nanocomposite material, which could alleviate tumor hypoxia, promote radiation-induced DNA damage, and ultimately inhibit tumor growth *in vivo*.

Except for Gd, Hf and Ce based nano-radiosensitizers, some other rare earth elements such as europium (Eu) and yttrium (Y) containing nanoparticles were also used for radiosensitization. Ghaemi *et al.*<sup>76</sup> doped high Z elements Eu and Gd into zinc oxide (ZnO) nanoparticles. The results showed that the therapeutic effect of 20  $\mu$ g mL<sup>-1</sup> of nanoparticles at 2 Gy of X-ray dose was the same as that of untreated cells under 6 Gy X-ray irradiation. The efficiency of intracellular X-ray was improved effectively. Porosnicu *et al.*<sup>77</sup> studied the radiotherapy effect of Y<sub>2</sub>O<sub>3</sub> nanoparticles combined with X-ray irradiation on A375 melanoma cells. The DNA damage of cells exposed to 50  $\mu$ g mL<sup>-1</sup> of Y<sub>2</sub>O<sub>3</sub> nanoparticles was more severe than that of 6 Gy X-ray dose irradiation alone. Notably, Liu *et al.*<sup>78</sup> constructed a multifunctional nano-radiosensitizer with the

under conversion nanoparticles (UCNPs) as the core. The UCNPs core was used as a radiation dose amplifier, a multifunctional matrix for bioimaging, and a near-infrared control/MR monitoring of drug release. It has the potential to be further developed into a powerful platform for future multi-modal imaging-guided therapy.

## 4. Semiconductor metal-based nano-radiosensitizers

The conductivity of a semiconductor is between an insulator and a conductor, and it may greatly change the stimulation under external light and heat. Therefore, semiconductor materials have great potential in the application of radiotherapy sensitization. Semiconductor nanomaterials with photocatalytic function could be activated by light to produce free radicals and enhance the radiation effect.<sup>78</sup>

The metal element Bi has the highest atomic number among all non-radioactive elements and possesses excellent radiosensitization.<sup>79</sup> Bi-containing semiconductors such as Bi<sub>2</sub>S<sub>3</sub>, Bi<sub>2</sub>Se<sub>3</sub> and Bi<sub>2</sub>O<sub>3</sub> have the advantages of small carrier effective masses, long Fermi wavelength, and small band overlap energy, are popular materials in the field of radiosensitization.<sup>80-83</sup> In addition, studies have shown that Bi is not only an excellent photothermal material, but can also be used for computed tomography (CT) as a radiosensitizer and a contrast agent.<sup>84</sup> Bi-based nanomaterials could utilize the high-Z element Bi to block X-rays and interact with and deplete GSH, thereby increasing X-ray deposition at tumor sites and enhancing RT.<sup>85,86</sup> Yu *et al.*<sup>10</sup> constructed Bi-LyP-1 NPs based on peptide (LyP-1) labeled ultra-small Bi NPs with a diameter of about 3.6 nm. The ability of Bi element to absorb ionizing radiation and radiation under the second near-infrared laser (NIR-II 1064 nm) enabled the Bi-LyP-1 NPs to perform dual-mode photoacoustic/CT imaging and highly coordinated NIR-II tumor photothermal/radio-therapy. The survival score of cells treated with Bi-LyP-1 NPs at 4 Gy was about 0.107, which improves the efficacy of radiotherapy significantly. In addition, Bi-LyP-1 NPs could be completely eliminated from the mouse's body *via* urine and faeces after 30 days. This is the first report on the photothermal and radiation properties of Bi NPs and their applications in biomedical and multimodal imaging. However, the easy oxidation of Bi nanocrystals hindered their development. To solve this problem, Yu *et al.*<sup>87</sup> used the chemical reduction method to coat Bi NPs with thiol ligands and modified them with polyethylene glycol phospholipids on their surfaces. Because the adsorption energy between metal and sulfur was enhanced, thiol ligands on the surface of Bi-SR-PEG were able to remarkably avoid the nuclear oxidation of Bi. Importantly, under the irradiation of 4 Gy X-ray dose, the survival rate of tumor cells in the injected nanoparticle group was half of that in the blank control group, indicating Bi NPs have a significant photosensitization effect and could absorb and concentrate the radiation dose. Cheng *et al.*<sup>81</sup> prepared Bi<sub>2</sub>S<sub>3</sub> nanoagents; both *in vivo* and *in vitro* experiments



confirmed that  $\text{Bi}_2\text{S}_3$  nanoagents could improve the anti-tumor effect of RT by enhancing the local radiation dose and photo-thermal effect, thus increasing the lethal effect of radiation. In addition, these nanoagents also have the ability to act as contrast agents for X-ray, CT and photoacoustic imaging. Subsequently, Ren *et al.*<sup>88</sup> doped ultra-small  $\text{Bi}_2\text{S}_3$  quantum dots into hollow mesoporous Prussian blue (HMPB) nanocubes to amplify tumor oxidative stress and enhance light/radiotherapy. Ultra-small  $\text{Bi}_2\text{S}_3$  quantum dots could not only be used in CT and RT with obvious therapeutic effects, but also prolong blood circulation and reduce systemic toxicity of kidney metabolism. Du *et al.*<sup>89</sup> used a hydrothermal method to synthesize hyaluronic acid functionalized bismuth oxide nanoparticles (HA- $\text{Bi}_2\text{O}_3$  NPs) for targeted CT imaging and radiosensitization of tumors. Song *et al.*<sup>90</sup> prepared PEG- $\text{Bi}_2\text{Se}_3$ @PFC@ $\text{O}_2$  nanoparticles. Experiment showed the cancer cells treated with PEG- $\text{Bi}_2\text{Se}_3$  + RT exhibited remarkably enhanced DNA damage compared to those treated with RT and PEG- $\text{Bi}_2\text{Se}_3$  alone. In addition, further enhanced DNA damage was induced by PEG- $\text{Bi}_2\text{Se}_3$ @PFC@ $\text{O}_2$  + RT, to a level even higher than that achieved by PEG- $\text{Bi}_2\text{Se}_3$  + RT. On the one hand, Bi as a high-Z element can effectively concentrate a greater local radiation dose within the tumor, thus enhancing the RT efficacy to cancer. On the other hand, PFC loaded inside these hollow nanoparticles could be used as an oxygen carrier to moderately improve tumor oxygenation during NIR laser irradiation and further overcome the hypoxia-associated radio-resistance of tumors. As shown in Fig. 4, Yao *et al.*<sup>80</sup> used bovine serum albumin as a template to prepare  $\text{Bi}_2\text{Se}_3$ - $\text{MnO}_2$  nanocomposites. The nanocomposites were used as radiosensitizers to increase the local radiation dose, and showed excellent performance in CT and

MRI. Similarly, Liu *et al.*<sup>91</sup> encapsulated bismuth (Bi)-based nanospheres in the  $\text{MnO}_2$  layer to form a core-shell-structured radiosensitizer (Bi@Mn), and then loaded docetaxel (DTX). The biodegradable composite Bi@Mn-DTX-PFA could simultaneously modulate TME and achieve multimodal treatment (RT/CDT/CHT) for hypoxic tumors. Song *et al.*<sup>92</sup> designed  $\text{MnSe}@\text{Bi}_2\text{Se}_3$  core-shell nanostructures by a partial cation exchange method. The  $\text{Bi}_2\text{Se}_3$  shell endowed the nanostructure with strong absorbance of both X-rays and NIR light, which was useful for computed tomography (CT) imaging, enhanced RT, as well as PTT. A remarkably enhanced DNA damage level induced by X-rays (4 Gy) was observed on cancer cells treated with  $\text{MnSe}@\text{Bi}_2\text{Se}_3$ -PEG in comparison to the PBS control; the SER of  $\text{MnSe}@\text{Bi}_2\text{Se}_3$ -PEG was calculated to be 1.16, suggesting the strong RT enhancement effect of the Bi-containing nanoparticles. In recent years, Bi element based heterostructures also attracted much attention. Wang *et al.*<sup>93</sup> proposed a metal-semiconductor heterostructure based on the Schottky barrier (Au- $\text{Bi}_2\text{S}_3$  HNSCs). As a radiosensitizer, it could not only deposit a higher radiation dose in the tumor in the form of high-energy electrons, but also generate a large number of low-energy electron-hole pairs triggered by X-rays. Moreover, it could use the catalytic reaction triggered by X-rays to effectively decompose  $\text{H}_2\text{O}_2$  over-expressed in the tumor microenvironment into highly toxic  $\cdot\text{OH}$  to enhance the effect of selective radiotherapy in hypoxic tumors. Under X-ray irradiation, the  $\gamma$ -H2AX fluorescent spots of cells treated with Au- $\text{Bi}_2\text{S}_3$  HNSCs increased significantly, which was 5.65 times that of cells treated with X-rays alone. Moreover, colonies formed by Au- $\text{Bi}_2\text{S}_3$  HNSCs treated HeLa cells decreased sharply from 80% to 15% under X-ray irradiation, reflecting the high efficiency of

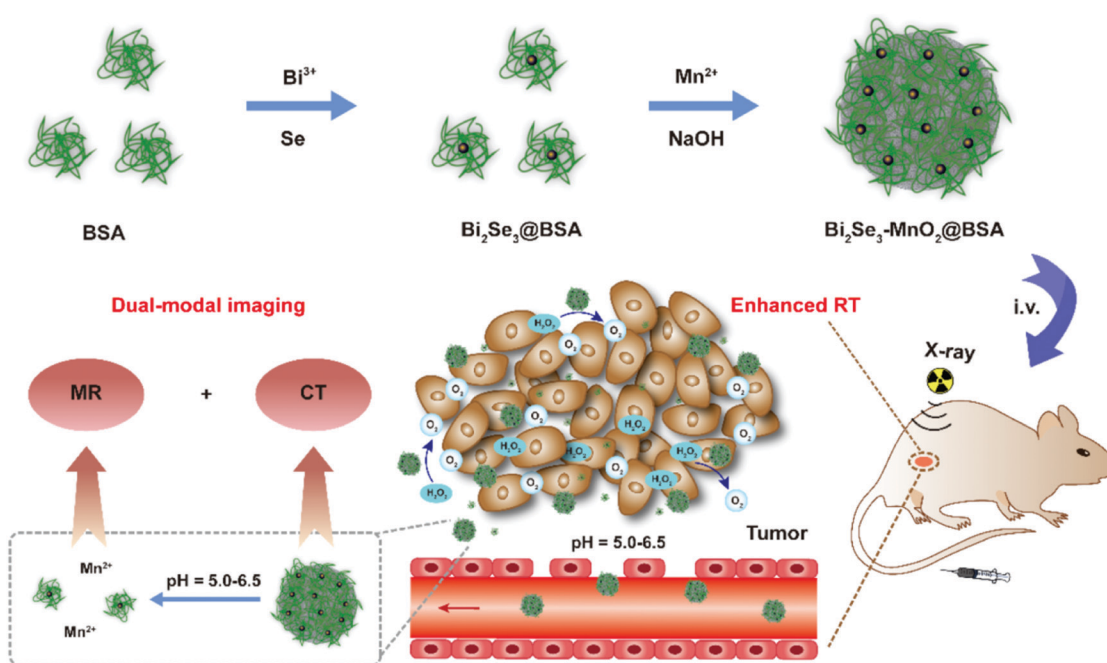


Fig. 4 Synthetic schematic of  $\text{Bi}_2\text{Se}_3$ - $\text{MnO}_2$ @BSA NPs and their application in enhanced RT. Copyright © 2021 American Chemical Society. Reprinted from ref. 80 with permission.



Au–Bi<sub>2</sub>S<sub>3</sub> HNSCs as radiosensitizers. The catalytic process of Au–Bi<sub>2</sub>S<sub>3</sub> HNSCs triggered by X-rays did not require oxygen and provided an easy and effective method to produce non-oxygen dependent free radicals in hypoxic tumors, which provided a new idea for the rational design of effective radiosensitizers.

It is important to note that Bi is more suitable for *in vivo* applications due to its low toxicity, good biocompatibility, and higher cost-effectiveness than other high-altitude ordinal elements.<sup>83,94</sup> In addition, Bi also has good reactivity and solubility. The size and shape of its particles in the process of synthesis are easy to control and they can be easily eliminated from the body.<sup>95</sup> They are also used in off-the-shelf drugs (e.g. Pepto-Bismol),<sup>96</sup> which confirmed their relative safety. Therefore, Bi NPs are a very promising multi-mode nanoplatform for dual-mode CT/PA guided combination therapy. Zang *et al.*<sup>97</sup> synthesized polyvinylpyrrolidone (PVP) modified Bi<sub>2</sub>WO<sub>6</sub> nanosheets with good biocompatibility; it was also the first time to be used in radiotherapy as a radiosensitizer. The high-Z elements Bi (Z = 83) and W (Z = 74) endowed PVP–Bi<sub>2</sub>WO<sub>6</sub> with better X-ray energy deposition performance, thereby enhancing the radiation damage. Besides, the Bi<sub>2</sub>WO<sub>6</sub> semiconductor exhibited obvious photocurrent and photocatalytic radiation catalytic activity under X-ray irradiation, leading to the effective separation of electron/hole pairs, thereby promoting the production of ROS and •OH. PVP–Bi<sub>2</sub>WO<sub>6</sub> nanosheets displayed excellent enhancement of radiotherapy efficacy in animal models, and could be used as an excellent contrast agent for X-ray CT imaging. These findings may provide another nanotechnology strategy for simultaneous radiation energy deposition and radiocatalytic tumor radiosensitization.

Being nontoxic and bio-inert, tantalum (Ta) has been widely used in clinical implants, artificial joints, and stents.<sup>98–100</sup> Ta is known to strongly absorb X-rays, so radiation energy can be deposited within the tumor to sensitize RT.<sup>101</sup> Many research studies focused on investigating the radiosensitization of tantalum oxide (TaOx).<sup>102,103</sup> Chen *et al.*<sup>104</sup> fabricated mesoporous tantalum oxide (mTa<sub>2</sub>O<sub>5</sub>) nanoparticles with PEG modification to allow efficient loading of doxorubicin (DOX). Since Ta possessed high X-ray attenuation coefficient, mTa<sub>2</sub>O<sub>5</sub>–PEG/DOX nanoparticles could offer an intrinsic radiosensitization effect to increase X-ray-induced DNA damage during radiotherapy. The nanoparticles could not only offer a significant radiosensitization effect, but also show dramatically reduced systemic toxicity compared to conventional chemoradiotherapy using free DOX. Song *et al.*<sup>105</sup> developed a simple and mild method to encapsulate catalase into hollow TaOx nanospheres (TaOx@Cat–PEG) as bio-nanoreactors. TaOx@Cat–PEG exhibited a RT enhancement effect, which was attributed to the factors that: (1) the Ta element could enable the deposition of radiation energy within the tumor to sensitize RT; (2) the catalase loaded inside TaOx nanospheres could effectively improve tumor oxygenation by decomposing endogenic H<sub>2</sub>O<sub>2</sub> in the tumor microenvironment, further overcoming the hypoxia-associated radio-resistance of tumors. Moreover, Song *et al.*<sup>106</sup> fabricated polyethylene glycol (PEG) stabilized perfluorocarbon (PFC) nano-droplets decorated with TaOx

nanoparticles (TaOx@PFC–PEG), and Gong *et al.*<sup>107</sup> prepared the core–shell TaOx@MnO<sub>2</sub> nanostructures for RT enhancement. The two studies also improved radiosensitivity through the accumulation of TaOx in X-rays and the increase of oxygen content in the tumor microenvironment. Furthermore, Peng *et al.*<sup>108</sup> constructed an oxygen-carrying nanoplatform based on polyethylene glycol TaOx (HMTCP@PFP) for triple sensitized tumor RT. O<sub>2</sub> would release when HMTCP@PFP was triggered by a near-infrared laser, which would improve the efficiency of radiotherapy. Meanwhile, radiant energy would be deposited inside the tumor by the Ta element, resulting in the reduction of the survival fractions of 4T1 cells after combined treatment (HMTCP@PFP@O<sub>2</sub> + RT) to 23.4%.

## 5. Other metal-based nano-radiosensitizers

Ti is considered to be a rare metal that is widely used in the medical field, especially in surgical applications, such as dental repair, human bone and tissue transplantation, *etc.*<sup>109–111</sup> Ti dioxide (TiO<sub>2</sub>) has been widely used in cancer treatment due to its high ionization energy conversion efficiency, larger surface area, low cytotoxicity and ultraviolet radiation absorption ability.<sup>112,113</sup> Studies have shown that TiO<sub>2</sub>-NPs could generate free radicals after irradiation, promoting the spontaneous production of ROS, thereby destroying nucleic acids (e.g., DNA).<sup>114–116</sup> Youkhana *et al.*<sup>117</sup> proved that TiO<sub>2</sub>-NPs are cyto-compatible to cells, even at very high concentrations. Incubation of prostate cancer and keratinocyte cell lines with TiO<sub>2</sub>-NPs could achieve significant radiosensitization. Pan *et al.*<sup>118</sup> developed nuclear targeted mesoporous TiO<sub>2</sub> nanoparticles (MTiO<sub>2</sub>(SN-38)–TAT–RGD), in which TiO<sub>2</sub> acted as a radiosensitizer to control the cancer cell cycle in the G<sub>2</sub>/M phase and enhance the lethality of radiation therapy to cancer cells. Followed by this, Pan's group<sup>119</sup> modified the core–shell structure of TiO<sub>2</sub>@MnO<sub>2</sub> with glucose oxidase (Gox), which could also effectively prevent the formation of lung metastases and prolong the survival rate of mice. Later, Morita *et al.*<sup>120</sup> designed the polyacrylic acid modified nano-titanium dioxide nanoparticles (PAA–TiO<sub>2</sub> NPs), which could strengthen the therapeutic effect of X-ray irradiation when used for local injection of tumors. PAA–TiO<sub>2</sub> NPs could also serve as carriers of H<sub>2</sub>O<sub>2</sub> to transport and continuously release H<sub>2</sub>O<sub>2</sub> in cells for at least 7 hours to keep H<sub>2</sub>O<sub>2</sub> at a high level. Thus, the radiosensitivity of tumor cells to X-rays was improved. Hou *et al.*<sup>121</sup> synthesized a nano-titanium dioxide composited polyurethane/polyacrylamide (TPU/PAAM) hydrogel and made it into pills. The results showed that the dose distribution of the TPU/PAAM group in the target area was much better than that in the commercial injection group, and sufficient dose was located at the lesion site. TPU/PAAM also had an antibacterial effect, which could produce better curative effects on superficial tumors.

Other common metal types with nano-radiosensitivity include iron (Fe) based and copper (Cu) based nano-radiosensitizers,



which could also catalyze the  $\text{H}_2\text{O}_2$  substrate to produce ROS. The sensitization mechanism of Cu-based nanoparticles is as follows:<sup>122</sup>  $\text{Cu}^{2+} + \text{H}_2\text{O}_2 \rightarrow \text{Cu}^+ + \text{HOO}^- + \text{H}^+$  (1);  $\text{Cu}^+ + \text{H}_2\text{O}_2 \rightarrow \text{Cu}^{2+} + \text{HO}^- + \text{OH}^-$  (2). Zhang *et al.*<sup>123</sup> designed an intelligent radiosensitizer based on  $\text{Cu}_2(\text{OH})\text{PO}_4$  nanocrystalline ( $\text{Cu}_2(\text{OH})\text{PO}_4$  @ PAAS NCs), which could respond to both exogenous stimuli (X-rays) and endogenous stimuli ( $\text{H}_2\text{O}_2$ ). After X-ray irradiation,  $\text{Cu}_2(\text{OH})\text{PO}_4$  nanocrystals would undergo photoelectron transfer to generate  $\text{Cu}^1$  positions. Under Fenton reaction,  $\text{Cu}^1$  sites triggered by X-rays play a role as a catalyst to effectively decompose  $\text{H}_2\text{O}_2$  overexpressed in TME into highly toxic hydroxyl radicals, which ultimately induced tumor cell apoptosis and necrosis. This ensured that the radiosensitization process was performed only in the hypoxic tumor and not in normal cells, thus effectively reducing the damage to the surrounding healthy tissue. Similarly, Fan *et al.*<sup>124</sup> proposed a nanoplatform

(G5.NHAc-Pyr/Cu(II)) based on the complexation of pyridine (Pyr) and 5th generation (G5) polyamide (PAMAM) dendrimers with Cu(II) (Fig. 5a), which could effectively enhance radiotherapy. After 22 days of treatment, the relative volume of tumor showed in Fig. 5b and c. The order of tumor size was G5.NHAc-Pyr/Cu(II) + RT ( $2.91 \pm 0.63$  times) < G5.NHAc-Pyr/Cu(II) ( $4.66 \pm 0.59$  times) < NS + RT ( $8.19 \pm 1.12$  times) < NS ( $10.56 \pm 0.57$  times). This is the first report of PAMAM dendrimers-coordinated Cu(II) complexes for tumor nanotherapy and metastasis. In order to maximize the multimodal imaging and therapeutic effects of nanomaterials, a variety of ways have been designed. Among them, the formation of heterostructures was of great interest, because the heterostructures not only exhibited the characteristics of individual components, but also had synergistic properties. Huang *et al.*<sup>125</sup> designed dumbbell-shaped multiphase nanocrystalline copper selenide gold (CSA), which could be used as an

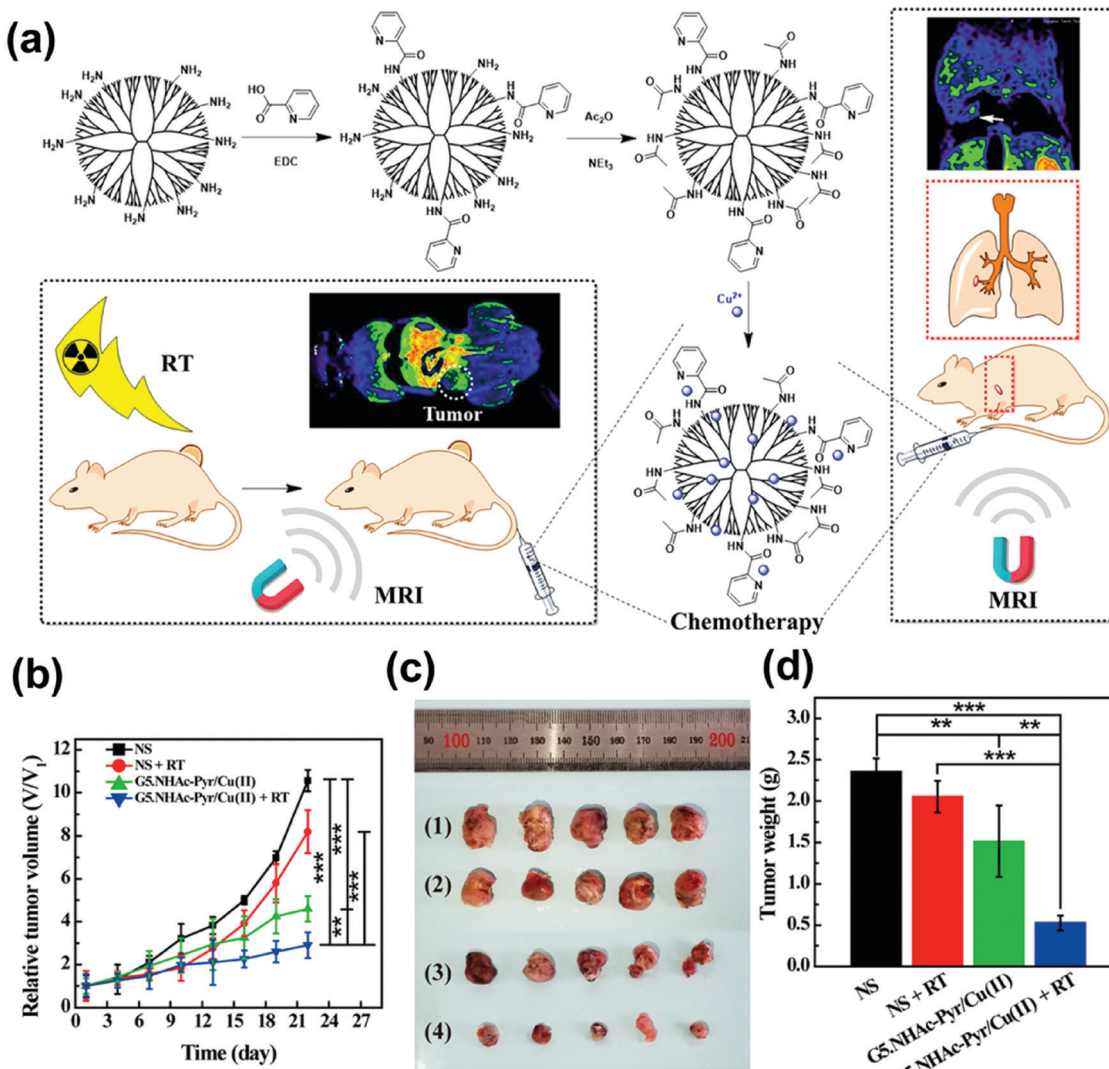


**Fig. 5** (a) Synthetic schematic of Cu(II) complexes with Pyr-functionalized PAMAM dendrimers for the RT-enhanced T1 MR imaging and chemotherapy of tumors and tumor metastasis; (b) the relative tumor volumes in 22 days after various treatments ( $n = 5$  in each group); (c) representative photographs of tumor tissues in (1) NS group, (2) NS plus RT group, (3) G5.NHAc-Pyr/Cu(II) group, and (4) G5.NHAc-Pyr/Cu(II) plus RT group; and (d) the average tumor weight. Copyright © 2019 American Chemical Society. Reprinted from ref. 124 with permission.



effective radiosensitizer, and this heterogeneous structure showed significant radiosensitization. Studies have showed that CuO nanoparticles are able to generate oxygen after microwave radiation, which obviously improves the oxygen concentration and oxygen pressure in TME, allowing tumor hypoxic cells to reoxygenize.<sup>126</sup> Chen *et al.*<sup>127</sup> reported that microwave (MW)-excited IL-Quercetin-CuO-SiO<sub>2</sub>@ZrO<sub>2</sub>-PEG nanoparticles (IQuCS@Zr-PEG NSPs) could uninterruptedly produce oxygen after microwave irradiation. After 20 min of microwave irradiation, the oxygen concentration produced was 3.10 times that of bare solution (phosphate buffered brine, PBS), improving the reoxygenation ability of the tumor, thereby enhancing the combined effect of radiotherapy and microwave hyperthermia.

Some iron (Fe)-based nano-radiosensitizers have also been reported. The sensitization mechanism of Fe-based NPs is as follows:<sup>128</sup>  $\text{Fe}^{2+} + \text{H}_2\text{O}_2 \rightarrow \text{Fe}^{3+} + \text{HO}^\cdot + \text{OH}^-$  (1);  $\text{Fe}^{3+} + \text{H}_2\text{O}_2 \rightarrow \text{Fe}^{2+} + \text{HOO}^\cdot + \text{H}^+$  (2). Yang *et al.*<sup>129</sup> developed a multifunctional hyperthermia system (Ge11-PDA-Pt@USPIOS) by wrapping ultra-small and super-paramagnetic iron oxide nanoparticles with polyacrylic acid. It exhibited synergistic therapeutic effects of radiotherapy and chemotherapy under low-temperature conditions *in vitro*. This study was also the first one to demonstrate that USPIO could alleviate tumor hypoxia and enhance tumor sensitivity to radiotherapy. Meidanchi *et al.*<sup>130</sup> used a hydrothermal reaction method to prepare superparamagnetic spinel zinc ferrite nanoparticles (ZnFe<sub>2</sub>O<sub>4</sub> NPs) as a radiosensitizer for tumor treatment. External radiotherapy of ZnFe<sub>2</sub>O<sub>4</sub> NPs on human prostate cancer cells (as a model of highly radiation-resistant cells) under  $\gamma$  ray irradiation showed that their killing rate for highly radiation-resistant cells was 17 times higher than that of radiotherapy alone. The highly biocompatible ZnFe<sub>2</sub>O<sub>4</sub> NPs (at a concentration of 100  $\mu\text{g mL}^{-1}$ ) had a synergistic effect in radiotherapy and were a reliable radiosensitizer. Shetake *et al.*<sup>131</sup> prepared iron oxide nanoparticles with oleic acid function (MN-OA). In MN-OA and radiation-treated cells, long lasting DNA damage could always be observed in the form of  $\gamma$ -H2AX lesions. Results showed that the cytotoxicity of the combination therapy (MN-OA + 2 Gy) was 3–5 times stronger than that of 2 Gy of radiation alone. The mechanism and effect of MN-OA induced radiosensitization was also verified in immunoactive mouse fibrosarcoma models. Hauser *et al.*<sup>128</sup> proved that iron oxide nanoparticles could be utilized to enhance the effect of radiation *via* ROS. Fakhimikabir *et al.*<sup>132</sup> prepared folic acid-conjugated polyglycerol coated iron oxide nanoparticles (FA-PG-SPIONs). Results revealed that higher concentrations of the FA-PG-SPIONs (200  $\mu\text{g mL}^{-1}$ ) in combination with 6 MeV electron beams could enhance radiosensitization of HeLa cells. Jafari *et al.*<sup>133</sup> studied the radiosensitization of polyglycerol coated superparamagnetic iron oxide nanoparticles (PG-SPIONs) on U87-MG cancer cells. The results showed that compared with radiotherapy alone, the survival rate of U87-MG cells was significantly decreased by PG-SPIONs + 6 MV X-rays. Studies have shown that clinically relevant radiotherapeutic isotopes (such as <sup>(223)</sup>Ra, <sup>(213)</sup>Bi, <sup>(177)</sup>Lu, <sup>(90)</sup>Y, <sup>(89)</sup>Zr, <sup>(67)</sup>Cu and <sup>(64)</sup>Cu) marked superparamagnetic iron oxide nanoparticles

could lead to enhanced localized submicron radiation damage with up to 20% increase in radiation dose.<sup>134</sup>

Tungsten (W) is able to emit photoelectrons, scattered photons, Compton electrons, negative electron pairs and positron, and Auger electrons under high energy irradiation to produce radiochemicals (free radicals and ionization) that kill tumor cells.<sup>1</sup> Wang *et al.*<sup>135</sup> demonstrated that tungsten sulfide quantum dots (WS<sub>2</sub> QDs) could be used for photothermal therapy (PTT) and RT. Dong *et al.*<sup>136</sup> designed semiconductor heterojunction structured WO<sub>2.9</sub>-WSe<sub>2</sub>-PEG nanoparticles. Under X-ray irradiation, the nanosystem could catalyze the high expression of H<sub>2</sub>O<sub>2</sub> in TME to produce oxygen-independent ROS. The results showed that local RT/PTT under low radiation dose and mild temperature was able to efficiently inhibit tumor metastasis, ablate local tumors, and prevent recurrence of tumors. At the same time, the nanosystem could also induce high temperature under near-infrared irradiation to enhance RT results.

Molybdenum (Mo) has a high Z number and has also been used as a radiosensitizer in radiotherapy. Wang *et al.*<sup>137</sup> synthesized MoS<sub>2</sub>@PANI multifunctional nanomaterials, which could effectively enhance radiation sensitivity and improve radiotherapy. Kirakci *et al.*<sup>138</sup> reported a new generation of RSs based on octahedral molybdenum cluster complexes (Mo<sub>6</sub>) that could directly produce O<sub>2</sub>(<sup>1</sup> $\Delta_g$ ) after exposure to X-rays. And it had evident radiotoxicity towards human cervix carcinoma HeLa and human MRC fibroblast cells. Another study by their group also confirmed that Mo<sub>6</sub> with iodine inner ligands could be efficiently quenched by oxygen to produce O<sub>2</sub>(<sup>1</sup> $\Delta_g$ ) during X-ray irradiation, and exhibited a noticeable radiotoxic effect against cancerous Hep-2 cells but negligible radiotoxic effect against normal MRC-5 cells.<sup>139</sup>

## 6. Non-metal-based nano-radiosensitizers

Black phosphorus (BP) is known as a supermaterial, which not only attracts wide attention in the fields of transistors, optoelectronic devices, catalysis, energy and so on, but also shines in the application in biological materials.<sup>140</sup> BP nanosheets were able to induce overproduction of <sup>1</sup>O<sub>2</sub> during X-ray irradiation, creating damage and apoptosis of nearby cancerous cells.<sup>141</sup> However, BP is easily oxidized into PxO<sub>y</sub> species at room temperature, which greatly limits its application prospects.<sup>142</sup> Zhang *et al.*<sup>143</sup> synthesized Pt@BP through surface coordination, and maintained the surface morphology and performance of BP nanosheets for more than 24 h at room temperature. Pt@BP showed good cell uptake rates compared to unmodified cisplatin. This study was the first attempt to stabilize BP with cationic cisplatin, providing a new way to alleviate the oxidation of BP. Huang *et al.*<sup>142</sup> synthesized the BP/Bi<sub>2</sub>O<sub>3</sub> heterostructure by the *in situ* growth method as a highly effective biocompatible sensitizer for tumor synergistic radiotherapy. The Bi<sub>2</sub>O<sub>3</sub> modification inhibited the rapid degradation of BP nanosheets and made the BP/Bi<sub>2</sub>O<sub>3</sub> heterojunction exhibit good stability in



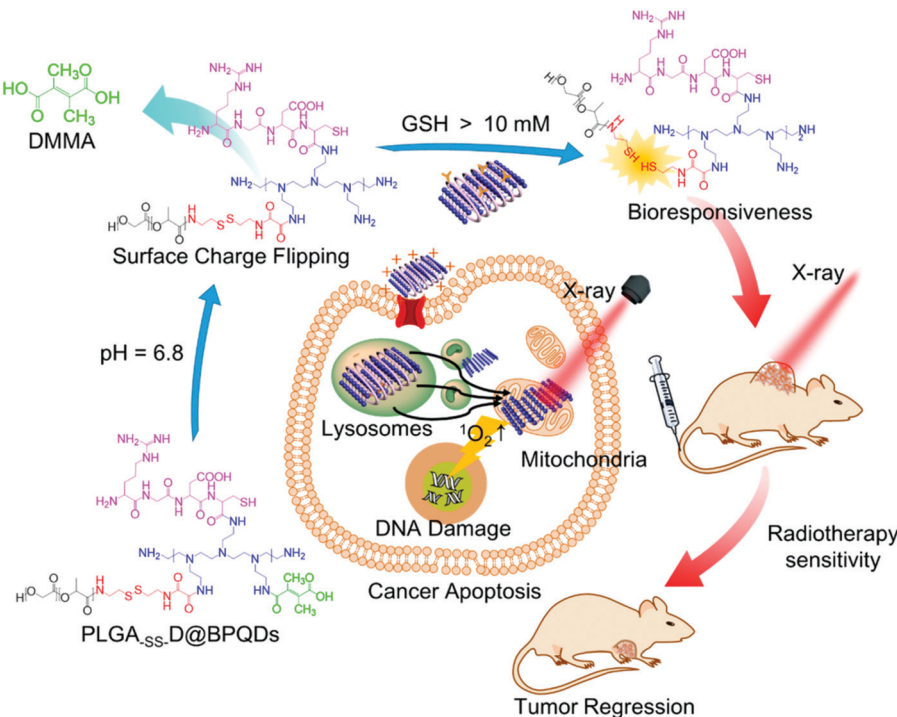


Fig. 6 Rational design and application of PLGA-SS-D@BPQDs to tumor radiotherapy. Copyright © 2018 American Chemical Society. Reprinted from ref. 144 with permission.

water. The synergistic effect of  $\text{Bi}_2\text{O}_3$  and BP triggered the excessive production of  ${}^1\text{O}_2$ , improving efficient X-ray photodynamic therapy effect, blocking cell cycle and inducing apoptosis. Similarly, Chan *et al.*<sup>144</sup> designed a nanosystem (PLGA-SS-D@BPQDs) based on poly (lactic-co-glycolic acid) and ultra-small black phosphorus quantum dots (BPQDs) for accurate tumor radiosensitization (Fig. 6). The singlet oxygen efficacy of PLGA-SS-D@BPQDs increased from 100% to 178% after X-ray irradiation. Therefore, the relative tumor volume on the 21st day after PLGA-SS-D@BPQDs and PLGA-SS-D@BPQDs + X-ray treatment reduced to 2168% and 1220%, while the relative tumor volume on the 21st day after the saline and X-ray treatment increased to 4279% and 3866%. These research studies indicated that there is great potential and research space for the application of materials containing BP nanostructures in biomedicine.

Selenium (Se) is an essential trace element in the human body.<sup>145</sup> In the past, Se has shown interesting radioprotective properties as a low toxic and potent antioxidant agent.<sup>146–150</sup> In recent years, Se has also been found to have radiosensitization,<sup>151</sup> and it exhibited a differential effect on the tumor and normal cells.<sup>152</sup> Cruz *et al.*<sup>153</sup> synthesized Se nanoparticles (SeNPs). MTT assay manifested that the synergistic effect of the SeNPs + X-ray played a key role on increasing cell killing through remarkably elevating caspase-3 activity to induce apoptosis and cell cycle arresting. SeNPs also showed potent cytotoxicity effect on cancer cells, but relatively less toxic effect on normal healthy cells. Furthermore, Chen *et al.*<sup>154</sup> evaluated the therapeutic effect of nano-Se as a novel

radiosensitizer. Nano-Se was applied in combination with radiation against McF-7 breast cancer cells. Results showed that nano-Se could enhance the toxic function on radiation, resulting in higher mortality than when used alone. Hence, nano-Se was expected to be used as an adjunct drug to increase the sensitivity of cancer cells to the toxic effects of radiation, thereby reducing the damage to nearby normal tissues. Later, Gao *et al.*<sup>155</sup> constructed a series of ionizing radiation-responsive NPs using Se-containing block co-polymers (PSeR/DOX). *In vitro* simulation experiments showed that when treated with PSeR NPs/5 Gy radiation, a remarkable reduction in the GSH/GSSG level was observed in MDA-MB-231 cells, the expression of catalase was increased and the intracellular ROS level was up-regulated from 55.3% to 85%. This treatment also down-regulated the expression of HLA-E and enhanced the NK cell-mediated cytotoxicity, demonstrating that Se-containing NPs not only had a sensitive response to radiation stimuli but also possessed potential anticancer effects and immune checkpoint inhibitor activity with radiotherapy. Similarly, Farhood *et al.*<sup>152</sup> also discussed the radiomitigative and radioprotective effects of selenium on normal cells/tissues, and its radiosensitive effect on cancer cells.

Quercetin is one of the main flavonoids, a secondary metabolite of plants, and a traditional Chinese medicine used for asthma, anti-allergic, antihypertensive and tumor treatments.<sup>156</sup> It has been reported that quercetin played an important role in tumor radiosensitivity, which can improve the radiosensitive effect by inhibiting the ATM mediated pathway whether *in vitro* or *in vivo*.<sup>157</sup> Huang *et al.*<sup>157</sup> used quercetin-loaded mesoporous

silica nanoparticles as a radiosensitizer. The results showed that the nanosystem could promote the apoptosis process in tumor cell and inhibit tumor growth whether *in vitro* or *in vivo*. However, the poor solubility of quercetin is an urgent problem to be solved. Ma *et al.*<sup>158</sup> proposed metal-organic framework (Zr-MOF-QU) nanoparticles based on quercetin (QU) modification, in which QU acted as a radiosensitizer, and Zr-MOF acted as both the raw material for the production of carbonic anhydrase IX (CAIX) inhibitor and the nano-carrier. QU was embedded in the Zr-MOF structure to increase the absorption of radiation energy and reduce the hypoxia conditions of tumor, so as to achieve synergic dual sensitization therapy. RT experimental results showed that the composite nanomaterial could reduce the resistance of tumor tissue to radiation injury and enhance the sensitivity of tumor tissue to radiation injury.

Imidazole compounds, especially nitroimidazole, are a kind of hypoxic cell radiosensitizing agent.<sup>159</sup> A variety of nitroimidazole radiotherapy sensitizers have been developed and used in clinical practice, such as pemonidazole, nimoprazole, and glycididazole sodium.<sup>160</sup> Liu *et al.*<sup>161</sup> combined the hypoxic radiosensitizer nitroimidazole with lipid molecules with hydrolyzable ester bonds to form MDH, and then mixed it with DSPE-PEG2000 and cholesterol to prepare MLP liposomes. The hypoxia radiosensitizer nitroimidazole increased the radiosensitivity of radiation-tolerant hypoxia cells through electron affinity and caused the DNA damage by ionizing radiation. Masunaga *et al.*<sup>162</sup> compared the radiosensitizing effect of the radiosensitizing agents on three hypoxic cells (SCC VII, SAS/neo and SAS/mp53 tumors) under aerobic and hypoxic conditions. The radiosensitization and repair inhibition of  $\alpha$ -ray irradiation under aerobic and hypoxia conditions were as follows: Nimorazole < SR-2514 < misonidazole. The combination of radiosensitizer and conventional radiotherapy showed good radiosensitization and repair inhibition in controlling radio-resistant Q tumor cells and p53 mutant tumor cells, but the toxicity of the radiosensitizing agents to normal tissues needed to be further studied.

Some other nonmetallic nanomaterials also have good radiosensitization effect. For example,  $\text{SiO}_2$  layers can enhance radiation sensitization by increasing ROS production. Fathy *et al.*<sup>163</sup> prepared silica coated magnetic iron oxide nanoparticles (SiO-MnPs), which were a promising engineering nanoagent for enhancing the radiosensitivity of breast cancer. This was the first study to evaluate the radiosensitization effect of silica coated iron oxide nanoparticles. But it lacked *in vivo* testing. Ruan *et al.*<sup>13</sup> prepared graphene quantum dots (GQDs) with a high oxidation degree, which were used for the first time in radiotherapy of colorectal cancer. Results showed that the synergistic effect of GQDs and ionizing radiation could improve G<sub>2</sub>/M phase arrest greatly, repress cell proliferation and promote cell apoptosis. It also led to excessive production of ROS, mitochondrial damage of tumor cells, activation of apoptosis-related regulatory proteins, and ultimately resulted in the apoptosis of tumor cells. 5-Iodine-2-deoxyuracil nucleoside (IUDR) has been shown to play an important role in radiosensitization of glioblastoma.<sup>164</sup> DNA double-strand repair

inhibitor (DSBRI) KU55933 was once deemed to be one of the most prospective drugs for improving radiotherapy, but its clinical application still encountered some problems due to its latent poisonous nature to normal tissues, inability to optionally enter tumor cells and poor solubility.<sup>165</sup>

## 7. Conclusions and prospects

The rapid development and application of nanomaterials in the biomedical field provide a good opportunity to improve the efficiency of radiotherapy. Through this review, we have comprehensively summarized the recent advances in nanotechnology in improving radiation therapy for cancers. Due to their unique properties, nanomaterials can play a key role in tumor radiation therapy in a number of different ways to overcome radiation resistance and enhance radiation response. According to the physical and chemical properties of their main elements, they mainly include nanomaterials containing precious metals; nanomaterials containing semiconductor metal elements; nanomaterials containing rare earth metal elements; nanomaterials containing other metal elements; and nanomaterials containing non-metallic elements (Table 1). Precious metal-based nano-radiosensitizers such as GNPs and AgNPs were reported to have low toxicity. However, the sensitization effect of GNPs depends on the shape and size of nanoparticles, the type of surface modifier and the shape of tumor cells. And the radiation sensitization mechanism of AgNPs may be more complex. Therefore, the potential for clinical translation of the GNPs and AgNPs needs more investigations. Rare earth metal-based nano-radiosensitizers (Gd, Hf, Ce *etc.*) have been widely used in biomedical fields due to their non-toxicity and good biocompatibility. In particular Gd-based radiosensitizers have been used in a variety of animals (including non-human primates) and tested in a variety of tumors, and they have great significance and potential for clinical translation. Semiconductor metal based nano-radiosensitizers such as Bi containing radiosensitizers have also been widely focused due to their low toxicity, good biocompatibility, excellent photothermal conversion ability and radiosensitization ability. But, the easy oxidation of Bi nanocrystals and the lack of in-depth research on Bi make their clinical transformation requiring further study. The toxicity of other metal elements (Ti, Cu, Fe, Ta *etc.*) and non-metal elements (BP, Se *etc.*) is also studied. Surprisingly, Se element based radiosensitizers exhibit differential effect on the tumor and normal cells and show interesting radioprotective properties and radiosensitization. We believe that the clinical application of selenium-based nano-radiosensitizers also should receive more attention.

To sum up, the effect of radiosensitization is affected by the size, shape, and modification method of the nanoparticles. The sensitization effect of the same nanomaterial to different cells under the same dose of radiation and the sensitization effect of the same cell under different doses are different. Therefore, there is a need to design nanoparticles with the best sensitization effect and corresponding size and shape for different



Table 1 Summary of the latest research progress of different types of nano-radiosensitizers

Main types	Main elements	Nano-sensitizers	Type and dose of radiation	SER value	Tumor cells	Ref.
Precious metal	Au	NH <sub>2</sub> -GNSS, FA-GNSS, TAT-GNSS	X-rays 4 Gy	2.30 (TAT-GNSS)	KB cancer cells	18
		GNPs, GNSS, GNRs	X-rays 4 Gy	1.62, 1.37, 1.21	KB cancer cells	19
		Au-Pt NPs	X-rays 4 Gy		U87-MG cells	22-24
	Ag	PAuNTs	X-rays 250 kVp		Glioma, Breast cancer, U251, C6 cells, <i>et al.</i>	26
		AgNPs	X-rays 0-8 Gy		C6 glioma cells	28-32
		AsNPs	X-rays 0-8 Gy		U251 cells	34
Rare earth metal	Gd	AgNPs@BSA-AS-VRP	X-rays 4 Gy	1.55	A549 cells	35
		GONs	Carbon ion radiation	1.10 (A549), 1.11 (NH1299), 1.20 (NH1650)	SKLC-6 cancer	44
		Gd-doped ZnO NPs	X-rays 6 mV	1.47 (10 µg mL <sup>-1</sup> ), 1.61 (20 µg mL <sup>-1</sup> )	H1299, U87-MG, HeLa cells, <i>et al.</i>	47
	Hf	AGuIXNPs	X-rays 2-8 Gy		B16-F10 cells	52-61
		MnTCPP-Hf-FA MOF NPs	X-rays 4 Gy		A549, RM-1 cells	64
		Hf-BPY-Fe NPs	X-rays 4 Gy	1.41 (Hf-BPY), 1.74 (Hf-BPY-Fe)	4T1 tumor cells	65
Semiconductor metal	Bi	Bi-LyP-1NPs	X-rays 4 Gy	1.218 (SERD <sub>0</sub> ), 1.248 (SER10)	4T1 tumor cells	10
		Bi-SR-PEG	X-rays 4 Gy		4T1 tumor cells	87
		Bi <sub>2</sub> S <sub>3</sub> Nanoagents	X-rays 4 Gy		4T1 tumor cells	81
	Ta	mTa <sub>2</sub> O <sub>5</sub> -PEG/DOX	X-rays 6 or 8 Gy		4T1 tumor cells	104
		TaOx@Cat-PEG	X-rays 0-8 Gy		4T1 tumor cells	105
		TaOx@MnO <sub>2</sub>	X-rays 0-8 Gy		4T1 tumor cells	107
Other metals	Ti	MTiO <sub>2</sub> (SN-38)-TAT-RGD NPs	X-rays		4T1-Luc cells	118
		PAA-TiOxNPs	X-rays 5 Gy		BxPC3 cells	120
	Cu	Cu <sub>2</sub> (OH)PO <sub>4</sub> @PAAS NCs	X-ray irradiation (voltage:50 KV, current: 75 µA)		HeLa cells	123
		G5.NHAc-Pyr/Cu(II)	X-rays 4 Gy or 6 MeV		4T1, KB cells	124
		GE11-PDA-Pt@USPIOs	γ-rays (Cs137, 662 keV) 4 and 6 Gy		H1299, MCF-7 cells	129
		PG-SPIIONs	X-rays 6 MV		U87-MG cells	133
Non-metal	Se	SeNPs	X-rays		Lung cancer	153
	BP	PLGA-ss-D@BPQDs	X-rays 2 or 4 Gy		A375, HeLa cells	144

tumor cells, as well as the specific preparation method of synthetic nanoparticles. Moreover, nanomaterials have enough time to function in the body due to their slow biodegradation ability, low metabolic rate and long-time retention. However, these properties also tend to cause them to accumulate in the organs of the body, especially in the liver and kidneys, thereby leading to health hazards. Therefore, aiming for clinical translation, it is necessary to improve the metabolic rate of nanomaterials in the body and design green, easily degradable nanomaterials with non-toxic and harmless degradation products.

## Conflicts of interest

There is no potential conflict of interest to declare.

## Acknowledgements

This work was supported by National Natural Science Foundation of China (81901896) and Young and Middle-aged Backbone Personnel Training Project of Fujian Health and Family Planning Commission (2021GGA043).

## References

1. J. F. Hainfeld, F. A. Dilmanian, D. N. Slatkin and H. M. Smilowitz, *J. Pharm. Pharmacol.*, 2008, **60**, 977-985.
2. C. Global Burden of Disease Cancer, C. Fitzmaurice, C. Allen, R. M. Barber, L. Barregard, Z. A. Bhutta, H. Brenner, D. J. Dicker, O. Chimed-Orchir, R. Dandona, L. Dandona, T. Fleming, M. H. Forouzanfar, J. Hancock, R. J. Hay, R. Hunter-Merrill, C. Huynh, H. D. Hosgood, C. O. Johnson, J. B. Jonas, J. Khubchandani, G. A. Kumar, M. Kutz, Q. Lan, H. J. Larson, X. Liang, S. S. Lim, A. D. Lopez, M. F. MacIntyre, L. Marczak, N. Marquez, A. H. Mokdad, C. Pinho, F. Pourmalek, J. A. Salomon, J. R. Sanabria, L. Sandar, B. Sartorius, S. M. Schwartz, K. A. Shackelford, K. Shibuya, J. Stanaway, C. Steiner, J. Sun, K. Takahashi, S. E. Vollset, T. Vos, J. A. Wagner, H. Wang, R. Westerman, H. Zeeb, L. Zeeckler, F. Abd-Allah, M. B. Ahmed, S. Alabed, N. K. Alam, S. F. Aldhahri, G. Alem, M. A. Alemayohu, R. Ali, R. Al-Raddadi, A. Amare, Y. Amoako, A. Artaman, H. Asayesh, N. Atnafu, A. Awasthi, H. B. Saleem, A. Barac, N. Bedi, I. Bensenor, A. Berhane, E. Bernabe, B. Betsu, A. Binagwaho, D. Boneya, I. Campos-Nonato, C. Castaneda-Orjuela, F. Catala-Lopez, P. Chiang, C. Chibueze, A. Chitheer, J. Y. Choi,



B. Cowie, S. Damtew, J. das Neves, S. Dey, S. Dharmaratne, P. Dhillon, E. Ding, T. Driscoll, D. Ekwueme, A. Y. Endries, M. Farvid, F. Farzadfar, J. Fernandes, F. Fischer, G. H. TT, A. Gebru, S. Gopalani, A. Hailu, M. Horino, N. Horita, A. Husseini, I. Huybrechts, M. Inoue, F. Islami, M. Jakovljevic, S. James, M. Javanbakht, S. H. H. Jee, A. Kasaeian, M. S. Kadir, Y. S. Khader, Y. H. Khang, D. Kim, J. Leigh, S. Linn, R. Lunevicius, H. M. A. El Razek, R. Malekzadeh, D. C. Malta, W. Marcenés, D. Markos, Y. A. Melaku, K. G. Meles, W. Mendoza, D. T. Mengiste, T. J. Meretoja, T. R. Miller, K. A. Mohammad, A. Mohammadi, S. Mohammed, M. Moradi-Lakeh, G. Nagel, D. Nand, Q. Le Nguyen, S. Nolte, F. A. Ogbo, K. E. Oladimeji, E. Oren, M. Pa, E. K. Park, D. M. Pereira, D. Plass, M. Qorbani, A. Radfar, A. Rafay, M. Rahman, S. M. Rana, K. Soreide, M. Satpathy, M. Sawhney, S. G. Sepanlou, M. A. Shaikh, J. She, I. Shiue, H. R. Shore, M. G. Shrimé, S. So, S. Soneji, V. Stathopoulou, K. Stroumpoulis, M. B. Stufyan, B. L. Sykes, R. Tabares-Seisdedos, F. Tadese, B. A. Tedla, G. A. Tessema, J. S. Thakur, B. X. Tran, K. N. Ukwaja, B. S. C. Uzochukwu, V. V. Vlassov, E. Weiderpass, M. Wubshet Terefe, H. G. Yebo, H. H. Yimam, N. Yonemoto, M. Z. Younis, C. Yu, Z. Zaidi, M. E. S. Zaki, Z. M. Zenebe, C. J. L. Murray and M. Naghavi, *JAMA Oncol.*, 2017, **3**, 524–548.

3 H. Sung, J. Ferlay, R. L. Siegel, M. Laversanne, I. Soerjomataram, A. Jemal and F. Bray, *Ca-Cancer J. Clin.*, 2021, **71**, 209–249.

4 Z. Li, Y. Gao, W. Li, Y. Li, H. Lv, D. Zhang, J. Peng, W. Cheng, L. Mei and H. Chen, *Smart Materials in Medicine*, 2022, **3**, 243–253.

5 K. Haume, S. Rosa, S. Grellet, M. A. Smialek, K. T. Butterworth, A. V. Solov'yov, K. M. Prise, J. Golding and N. J. Mason, *Cancer Nanotechnol.*, 2016, **7**, 8.

6 A. Z. Wang and J. E. Tepper, *J. Clin. Oncol.*, 2014, **32**, 2879–2885.

7 M. A. Hill, *Int. J. Radiat. Biol.*, 2018, **94**, 759–768.

8 R. Schulte, V. Bashkirov, G. Garty, C. Leloup, S. Shchemelinin, A. Breskin, R. Chechik, J. Milligan and B. Grosswendt, *Australas. Phys. Eng. Sci. Med.*, 2003, **26**, 149–155.

9 G. Song, L. Cheng, Y. Chao, K. Yang and Z. Liu, *Adv. Mater.*, 2017, **29**(32), 1700996.

10 X. Yu, A. Li, C. Zhao, K. Yang, X. Chen and W. Li, *ACS Nano*, 2017, **11**, 3990–4001.

11 S. Rockwell, I. T. Dobrucki, E. Y. Kim, S. T. Garrison and V. T. Vu, *Curr. Mol. Med.*, 2009, **9**(4), 442–458.

12 H. Huang, C. Zhang, X. Wang, J. Shao, C. Chen, H. Li, C. Ju, J. He, H. Gu and D. Xia, *Nano Lett.*, 2020, **20**, 4211–4219.

13 J. Ruan, Y. Wang, F. Li, R. Jia, G. Zhou, C. Shao, L. Zhu, M. Cui, D.-P. Yang and S. Ge, *ACS Appl. Mater. Interfaces*, 2018, **10**, 14342–14355.

14 E. K. Lim, T. Kim, S. Paik, S. Haam, Y. M. Huh and K. Lee, *Chem. Rev.*, 2015, **115**, 327–394.

15 Y. Yang, W. Zeng, P. Huang, X. Zeng and L. Mei, *View*, 2021, **2**, 20200042.

16 M. Hernandez-Rivera, I. Kumar, S. Y. Cho, B. Y. Cheong, M. X. Pulikkathara, S. E. Moghaddam, K. H. Whitmire and L. J. Wilson, *ACS Appl. Mater. Interfaces*, 2017, **9**, 5709–5716.

17 X. Yang, M. Yang, B. Pang, M. Vara and Y. Xia, *Chem. Rev.*, 2015, **115**, 10410–10488.

18 N. Ma, P. Liu, N. He, N. Gu, F.-G. Wu and Z. Chen, *ACS Appl. Mater. Interfaces*, 2017, **9**, 31526–31542.

19 N. Ma, F.-G. Wu, X. Zhang, Y.-W. Jiang, H.-R. Jia, H.-Y. Wang, Y.-H. Li, P. Liu, N. Gu and Z. Chen, *ACS Appl. Mater. Interfaces*, 2017, **9**, 13037–13048.

20 W. Sung, S.-J. Ye, A. L. McNamara, S. J. McMahon, J. Hainfeld, J. Shin, H. M. Smilowitz, H. Paganetti and J. Schuemann, *Nanoscale*, 2017, **9**, 5843–5853.

21 T. T. Jia, G. Yang, S. J. Mo, Z. Y. Wang, B. J. Li, W. Ma, Y. X. Guo, X. Chen, X. Zhao, J. Q. Liu and S. Q. Zang, *ACS Nano*, 2019, **13**, 8320–8328.

22 A. Kamkaew, F. Chen, Y. Zhan, R. L. Majewski and W. Cai, *ACS Nano*, 2016, **10**, 3918–3935.

23 S. Yang, G. Han, Q. Chen, L. Yu, P. Wang, Q. Zhang, J. Dong, W. Zhang and J. Huang, *Int. J. Nanomed.*, 2021, **16**, 239–248.

24 X. Liu, X. Zhang, M. Zhu, G. Lin, J. Liu, Z. Zhou, X. Tian and Y. Pan, *ACS Appl. Mater. Interfaces*, 2017, **9**, 279–285.

25 M. Shi, B. Paquette, T. Thippayamontri, L. Gendron, B. Guerin and L. Sanche, *Int. J. Nanomed.*, 2016, **11**, 5323–5333.

26 S. R. Bhattarai, P. J. Derry, K. Aziz, P. K. Singh, A. M. Khoo, A. S. Chadha, A. Liopo, E. R. Zubarev and S. Krishnan, *Nanoscale*, 2017, **9**, 5085–5093.

27 P. Liu, Z. Huang, Z. Chen, R. Xu, H. Wu, F. Zang, C. Wang and N. Gu, *Nanoscale*, 2013, **5**(23), 11829–11836.

28 R. Xu, J. Ma, X. Sun, Z. Chen, X. Jiang, Z. Guo, L. Huang, Y. Li, M. Wang, C. Wang, J. Liu, X. Fan, J. Gu, X. Chen, Y. Zhang and N. Gu, *Cell Res.*, 2009, **19**, 1031–1034.

29 R. Singh, J. Swanner, J. Mims, S. Akman, C. Furdui, S. Torti and D. Carroll, *Int. J. Nanomed.*, 2015, **10**, 3937–3953.

30 R. G. Saratale, H. S. Shin, G. Kumar, G. Benelli, D. S. Kim and G. D. Saratale, *Artif. Cells, Nanomed., Biotechnol.*, 2018, **46**, 211–222.

31 S. N. Sunil Gowda, S. Rajasowmiya, V. Vadivel, S. Banu Devi, A. Celestin Jerald, S. Marimuthu and N. Devipriya, *Toxicol. In Vitro*, 2018, **52**, 170–177.

32 L. Zhu, D. Guo, L. Sun, Z. Huang, X. Zhang, W. Ma, J. Wu, L. Xiao, Y. Zhao and N. Gu, *Nanoscale*, 2017, **9**, 5489–5498.

33 K. Habiba, K. Aziz, K. Sanders, C. M. Santiago, L. S. K. Mahadevan, V. Makarov, B. R. Weiner, G. Morell and S. Krishnan, *Sci. Rep.*, 2019, **9**(1), 1–9.

34 J. Zhao, P. Liu, J. Ma, D. Li, H. Yang, W. Chen and Y. Jiang, *Int. J. Nanomed.*, 2019, **14**, 9483–9496.

35 J. Zhao, D. Li, J. Ma, H. Yang, W. Chen, Y. Cao and P. Liu, *Nanotechnology*, 2021, **32**(14), 145102.

36 Z. Liu, H. Tan, X. Zhang, F. Chen, Z. Zhou, X. Hu, S. Chang, P. Liu and H. Zhang, *Artif. Cells, Nanomed., Biotechnol.*, 2018, **46**, S922–S930.

37 P. D. Liu, H. Jin, Z. Guo, J. Ma, J. Zhao, D. Li, H. Wu and N. Gu, *Int. J. Nanomed.*, 2016, **11**, 5003–5014.

38 Y. Liu, P. Zhang, F. Li, X. Jin, J. Li, W. Chen and Q. Li, *Theranostics*, 2018, **8**, 1824–1849.

39 W. Sun, Z. Zhou, G. Pratz, X. Chen and H. Chen, *Theranostics*, 2020, **10**, 1296–1318.



40 Z. Li, Y. Yang, H. Wei, X. Shan, X. Wang, M. Ou, Q. Liu, N. Gao, H. Chen and L. Mei, *J. Controlled Release*, 2021, **338**, 719–730.

41 A. Ku, V. J. Facca, Z. Cai and R. M. Reilly, *EJNMMI Radio-pharm. Chem.*, 2019, **4**, 27.

42 R. Mueller, M. Moreau, S. Yasmin-Karim, A. Protti, O. Tillement, R. Berbeco, J. Hesser and W. Ngwa, *Nanomaterials*, 2020, **10**(11), 2249.

43 S. Dufort, A. Bianchi, M. Henry, F. Lux, G. Le Duc, V. Josserand, C. Louis, P. Perriat, Y. Crémillieux and O. Tillement, *Small*, 2015, **11**, 215–221.

44 F. Li, Z. Li, X. Jin, Y. Liu, P. Li, Z. Shen, A. Wu, X. Zheng, W. Chen and Q. Li, *Nanoscale Res. Lett.*, 2019, **14**, 328.

45 C. Wu, R. Cai, T. Zhao, L. Wu, L. Zhang, J. Jin, L. Xu, P. Li, T. Li, M. Zhang and F. Du, *Nanoscale Res. Lett.*, 2020, **15**, 94.

46 T. Andoh, Y. Nakatani, M. Suzuki, Y. Sakurai, T. Fujimoto and H. Ichikawa, *Appl. Radiat. Isot.*, 2020, **164**, 109270.

47 M. Zangeneh, H. A. Nedaei, H. Mozdarani, A. Mahmoudzadeh and M. Salimi, *Mater. Sci. Eng., C*, 2019, **103**, 109739.

48 Z. Huang, Y. Wang, D. Yao, J. Wu, Y. Hu and A. Yuan, *Nat. Commun.*, 2021, **12**(1), 1–18.

49 W. Sun, L. Luo, Y. Feng, Y. Qiu, C. Shi, S. Meng, X. Chen and H. Chen, *Adv. Mater.*, 2020, **32**, e2000377.

50 C. Lee, X. Liu, W. Zhang, M. A. Duncan, F. Jiang, C. Kim, X. Yan, Y. Teng, H. Wang and W. Jiang, *Nanoscale*, 2021, **13**, 9252–9263.

51 X. Ma, C. Lee, T. Zhang, J. Cai, H. Wang, F. Jiang, Z. Wu, J. Xie, G. Jiang and Z. Li, *J. Nanobiotechnol.*, 2021, **19**, 1–10.

52 S. Dufort, G. Appelboom, C. Verry, E. L. Barbier, F. Lux, E. Brauer-Krisch, L. Sancey, S. D. Chang, M. Zhang, S. Roux, O. Tillement and G. Le Duc, *J. Clin. Neurosci.*, 2019, **67**, 215–219.

53 Y. Du, H. Sun, F. Lux, Y. Xie, L. Du, C. Xu, H. Zhang, N. He, J. Wang, Y. Liu, G. Leduc, T. Doussineau, K. Ji, Q. Wang, Z. Lin, Y. Wang, Q. Liu and O. Tillement, *ACS Appl. Mater. Interfaces*, 2020, **12**, 56874–56885.

54 C. Verry, L. Sancey, S. Dufort, G. Le Duc, C. Mendoza, F. Lux, S. Grand, J. Arnaud, J. L. Quesada, J. Villa, O. Tillement and J. Balosso, *BMJ Open*, 2019, **9**(2), e023591.

55 I. Miladi, M. T. Aloy, E. Armandy, P. Mowat, D. Kryza, N. Magne, O. Tillement, F. Lux, C. Billotey, M. Janier and C. Rodriguez-Lafrasse, *Nanomedicine*, 2015, **11**, 247–257.

56 P. Mowat, A. Mignot, W. Rima, F. Lux, O. Tillement, C. Roulin, M. Dutreix, D. Bechet, S. Huger, L. Humbert, M. Barberi-Heyob, M. T. Aloy, E. Armandy, C. Rodriguez-Lafrasse, G. Le Duc, S. Roux and P. Perriat, *J. Nanosci. Nanotechnol.*, 2011, **11**, 7833–7839.

57 M. Luchette, H. Korideck, M. Makrigiorgos, O. Tillement and R. Berbeco, *Nanomedicine*, 2014, **10**, 1751–1755.

58 A. Detappe, S. Kunjachan, L. Sancey, V. Motto-Ros, D. Biancur, P. Drane, R. Guieze, G. M. Makrigiorgos, O. Tillement, R. Langer and R. Berbeco, *J. Controlled Release*, 2016, **238**, 103–113.

59 S. Kotb, A. Detappe, F. Lux, F. Appaix, E. L. Barbier, V. L. Tran, M. Plissonneau, H. Gehan, F. Lefranc, C. Rodriguez-Lafrasse, C. Verry, R. Berbeco, O. Tillement and L. Sancey, *Theranostics*, 2016, **6**, 418–427.

60 F. Lux, V. L. Tran, E. Thomas, S. Dufort, F. Rossetti, M. Martini, C. Truillet, T. Doussineau, G. Bort, F. Denat, F. Boschetti, G. Angelovski, A. Detappe, Y. Crémillieux, N. Mignet, B. T. Doan, B. Larrat, S. Meriaux, E. Barbier, S. Roux, P. Fries, A. Muller, M. C. Abadjian, C. Anderson, E. Canet-Soulas, P. Bouziotis, M. Barberi-Heyob, C. Frochot, C. Verry, J. Balosso, M. Evans, J. Sidi-Boumedine, M. Janier, K. Butterworth, S. McMahon, K. Prise, M. T. Aloy, D. Ardail, C. Rodriguez-Lafrasse, E. Porcel, S. Lacombe, R. Berbeco, A. Allouch, J. L. Perfettini, C. Chargari, E. Deutsch, G. Le Duc and O. Tillement, *Br. J. Radiol.*, 2019, **92**, 20180365.

61 L. Sancey, F. Lux, S. Kotb, S. Roux, S. Dufort, A. Bianchi, Y. Crémillieux, P. Fries, J. L. Coll, C. Rodriguez-Lafrasse, M. Janier, M. Dutreix, M. Barberi-Heyob, F. Boschetti, F. Denat, C. Louis, E. Porcel, S. Lacombe, G. Le Duc, E. Deutsch, J. L. Perfettini, A. Detappe, C. Verry, R. Berbeco, K. T. Butterworth, S. J. McMahon, K. M. Prise, P. Perriat and O. Tillement, *Br. J. Radiol.*, 2014, **87**, 20140134.

62 M. H. Chen, N. Hanagata, T. Ikoma, J. Y. Huang, K. Y. Li, C. P. Lin and F. H. Lin, *Acta Biomater.*, 2016, **37**, 165–173.

63 L. R. H. Gerken, K. Keevend, Y. Zhang, F. H. L. Starsich, C. Eberhardt, G. Panzarasa, M. T. Matter, A. Wichser, A. Boss, A. Neels and I. K. Herrmann, *ACS Appl. Mater. Interfaces*, 2019, **11**, 437–448.

64 Y. Chen, H. Zhong, J. Wang, X. Wan, Y. Li, W. Pan, N. Li and B. Tang, *Chem. Sci.*, 2019, **10**, 5773–5778.

65 T. Gong, Y. Li, B. Lv, H. Wang, Y. Liu, W. Yang, Y. Wu, X. Jiang, H. Gao, X. Zheng and W. Bu, *ACS Nano*, 2020, **14**, 3032–3040.

66 J. Liu, F. Hu, M. Wu, L. Tian, F. Gong, X. Zhong, M. Chen, Z. Liu and B. Liu, *Adv. Mater.*, 2021, **33**(9), 2007888.

67 X. Zhong, X. Wang, G. Zhan, Y. a. Tang, Y. Yao, Z. Dong, L. Hou, H. Zhao, S. Zeng, J. Hu, L. Cheng and X. Yang, *Nano Lett.*, 2019, **19**, 8234–8244.

68 L. Sun, C. Jiang, W. Li, Z. He, G. Wang, C. Cheng, F. Chen, X. Fu, H. Jiang and Q. Sun, *J. Biomed. Nanotechnol.*, 2020, **16**, 1482–1494.

69 S. Singh, A. Kumar, A. Karakoti, S. Seal and W. T. Self, *Mol. BioSyst.*, 2010, **6**, 1813–1820.

70 G. Cheng, W. Guo, L. Han, E. Chen, L. Kong, L. Wang, W. Ai, N. Song, H. Li and H. Chen, *Toxicol. In Vitro*, 2013, **27**, 1082–1088.

71 M. S. Wason, J. Colon, S. Das, S. Seal, J. Turkson, J. Zhao and C. H. Baker, *Nanomedicine*, 2013, **9**, 558–569.

72 N. Abdi Goushbolagh, R. Abedi Firouzjah, K. Ebrahimnejad Gorji, M. Khosravanipour, S. Moradi, A. Banaei, A. Astani, M. Najafi, M. H. Zare and B. Farhood, *Artif. Cells, Nanomed., Biotechnol.*, 2018, **46**, S1215–S1225.

73 M. S. Wason, H. Lu, L. Yu, S. K. Lahiri, D. Mukherjee, C. Shen, S. Das, S. Seal and J. Zhao, *Cancers*, 2018, **10**(9), 303.

74 W. Jiang, X. Han, T. Zhang, D. Xie, H. Zhang and Y. Hu, *Adv. Healthcare Mater.*, 2020, **9**, e1901303.



75 X. Zhou, M. You, F. Wang, Z. Wang, X. Gao, C. Jing, J. Liu, M. Guo, J. Li, A. Luo, H. Liu, Z. Liu and C. Chen, *Adv. Mater.*, 2021, **33**, e2100556.

76 B. Ghaemi, O. Mashinchian, T. Mousavi, R. Karimi, S. Kharrazi and A. Amani, *ACS Appl. Mater. Interfaces*, 2016, **8**, 3123–3134.

77 I. Porosnicu, C. M. Butnaru, I. Tiseanu, E. Stancu, C. V. A. Munteanu, B. I. Bita, O. G. Dului and F. Sima, *Molecules*, 2021, **26**(11), 3403.

78 Y. Liu, Y. Liu, W. Bu, Q. Xiao, Y. Sun, K. Zhao, W. Fan, J. Liu and J. Shi, *Biomaterials*, 2015, **49**, 1–8.

79 F. Zhang, S. Liu, N. Zhang, Y. Kuang, W. Li, S. Gai, F. He, A. Gulzar and P. Yang, *Nanoscale*, 2020, **12**, 19293–19307.

80 Y. Yao, P. Li, J. He, D. Wang, J. Hu and X. Yang, *ACS Appl. Mater. Interfaces*, 2021, **13**, 28650–28661.

81 X. Cheng, Y. Yong, Y. Dai, X. Song, G. Yang, Y. Pan and C. Ge, *Theranostics*, 2017, **7**, 4087–4098.

82 G. Song, C. Liang, X. Yi, Q. Zhao, L. Cheng, K. Yang and Z. Liu, *Adv. Mater.*, 2016, **28**, 2716–2723.

83 M. A. Shahbazi, L. Faghfouri, M. P. A. Ferreira, P. Figueiredo, H. Maleki, F. Sefat, J. Hirvonen and H. A. Santos, *Chem. Soc. Rev.*, 2020, **49**, 1253–1321.

84 H. Xie, M. Liu, B. You, G. Luo, Y. Chen, B. Liu, Z. Jiang, P. K. Chu, J. Shao and X. F. Yu, *Small*, 2020, **16**, e1905208.

85 R. Zhou, H. Wang, Y. Yang, C. Zhang, X. Dong, J. Du, L. Yan, G. Zhang, Z. Gu and Y. Zhao, *Biomaterials*, 2019, **189**, 11–22.

86 Y. Li, Y. Sun, T. Cao, Q. Su, Z. Li, M. Huang, R. Ouyang, H. Chang, S. Zhang and Y. Miao, *Nanoscale*, 2017, **9**, 14364–14375.

87 N. Yu, Z. Wang, J. Zhang, Z. Liu, B. Zhu, J. Yu, M. Zhu, C. Peng and Z. Chen, *Biomaterials*, 2018, **161**, 279–291.

88 C. Ren, Y. Cheng, W. Li, P. Liu, L. Yang, Q. Lu, M. Xu, F. Tan, J. Li and N. Li, *Biomater. Sci.*, 2020, **8**, 1981–1995.

89 F. Du, J. Lou, R. Jiang, Z. Fang, X. Zhao, Y. Niu, S. Zou, M. Zhang, A. Gong and C. Wu, *Int. J. Nanomed.*, 2017, **12**, 5973–5992.

90 G. Song, C. Liang, X. Yi, Q. Zhao, L. Cheng, K. Yang and Z. Liu, *Adv. Mater.*, 2016, **28**, 2716–2723.

91 J. Liu, J. Zhang, K. Song, J. Du, X. Wang, J. Liu, B. Li, R. Ouyang, Y. Miao and Y. Sun, *Small*, 2021, **17**, 2101015.

92 G. Song, C. Liang, H. Gong, M. Li, X. Zheng, L. Cheng, K. Yang, X. Jiang and Z. Liu, *Adv. Mater.*, 2015, **27**, 6110–6117.

93 X. Wang, C. Zhang, J. Du, X. Dong, S. Jian, L. Yan, Z. Gu and Y. Zhao, *ACS Nano*, 2019, **13**, 5947–5958.

94 X. Ren, S. Yang, N. Yu, A. Sharjeel, Q. Jiang, D. K. Macharia, H. Yan, C. Lu, P. Geng and Z. Chen, *J. Colloid Interface Sci.*, 2021, **591**, 229–238.

95 J. Deng, S. Xu, W. Hu, X. Xun, L. Zheng and M. Su, *Biomaterials*, 2018, **154**, 24–33.

96 D. W. Bierer, *Rev. Infect. Dis.*, 1990, **12**(Suppl 1), S3–S8.

97 Y. Zang, L. Gong, L. Mei, Z. Gu and Q. Wang, *ACS Appl. Mater. Interfaces*, 2019, **11**, 18942–18952.

98 E. Koshevaya, E. Krivoshapkina and P. Krivoshapkin, *J. Mater. Chem. B*, 2021, **9**, 5008–5024.

99 C. Kang, L. Wei, B. Song, L. Chen, J. Liu, B. Deng, X. Pan and L. Shao, *Int. J. Nanomed.*, 2017, **12**, 4323.

100 M. Lu, S. Xu, Z.-X. Lei, D. Lu, W. Cao, M. Huttula, C.-H. Hou, S.-H. Du, W. Chen and S.-W. Dai, *Chin. Med. J.*, 2019, **132**, 51–62.

101 D. Ding, D. Zhang, F. He, G. Xie and Z. Chen, *Mater. Sci. Eng., C*, 2020, **110**, 110700.

102 N. Lee, H. R. Cho, M. H. Oh, S. H. Lee, K. Kim, B. H. Kim, K. Shin, T.-Y. Ahn, J. W. Choi and Y.-W. Kim, *J. Am. Chem. Soc.*, 2012, **134**, 10309–10312.

103 G. Song, Y. Chao, Y. Chen, C. Liang, X. Yi, G. Yang, K. Yang, L. Cheng, Q. Zhang and Z. Liu, *Adv. Funct. Mater.*, 2016, **26**, 8243–8254.

104 Y. Chen, G. Song, Z. Dong, X. Yi, Y. Chao, C. Liang, K. Yang, L. Cheng and Z. Liu, *Small*, 2017, **13**, 1602869.

105 G. Song, Y. Chen, C. Liang, X. Yi, J. Liu, X. Sun, S. Shen, K. Yang and Z. Liu, *Adv. Mater.*, 2016, **28**, 7143–7148.

106 G. Song, C. Ji, C. Liang, X. Song, X. Yi, Z. Dong, K. Yang and Z. Liu, *Biomaterials*, 2017, **112**, 257–263.

107 F. Gong, J. Chen, X. Han, J. Zhao, M. Wang, L. Feng, Y. Li, Z. Liu and L. Cheng, *J. Mater. Chem. B*, 2018, **6**, 2250–2257.

108 C. Peng, Y. Liang, Y. Chen, X. Qian, W. Luo, S. Chen, S. Zhang, Q. Dan, L. Zhang and M. Li, *ACS Appl. Mater. Interfaces*, 2019, **12**, 5520–5530.

109 S. El Hakim, T. Chave and S. I. Nikitenko, *Ultrason. Sonochem.*, 2021, **70**, 105336.

110 J. Jakubowicz, *Materials*, 2020, **13**(7), 1696.

111 N. E. Putra, M. J. Mirzaali, I. Apachitei, J. Zhou and A. A. Zadpoor, *Acta Biomater.*, 2020, **109**, 1–20.

112 W. Pan, B. Cui, P. Gao, Y. Ge, N. Li and B. Tang, *Chem. Commun.*, 2020, **56**, 547–550.

113 S. Cesmeli and C. Biray Avci, *J. Drug Targeting*, 2019, **27**, 762–766.

114 J. J. Yin, J. Liu, M. Ehrenshaft, J. E. Roberts, P. P. Fu, R. P. Mason and B. Zhao, *Toxicol. Appl. Pharmacol.*, 2012, **263**, 81–88.

115 M. Babaei and M. Ganjalikhani, *BioImpacts*, 2014, **4**, 15–20.

116 H. E. Townley, J. Kim and P. J. Dobson, *Nanoscale*, 2012, **4**, 5043–5050.

117 E. Q. Youkhana, B. Feltis, A. Blencowe and M. Geso, *Int. J. Med. Sci.*, 2017, **14**, 602–614.

118 W. Pan, S. Gong, J. Wang, L. Yu, Y. Chen, N. Li and B. Tang, *Chem. Commun.*, 2019, **55**, 8182–8185.

119 W. Pan, B. Cui, P. Gao, Y. Ge, N. Li and B. Tang, *Chem. Commun.*, 2020, **56**, 547–550.

120 K. Morita, Y. Nishimura, S. Nakamura, Y. Arai, C. Numako, K. Sato, M. Nakayama, H. Akasaka, R. Sasaki, C. Ogino and A. Kondo, *Colloids Surf., B*, 2021, **198**, 111451.

121 Y. Hou, Y. Song, X. Sun, Y. Jiang, M. He, Y. Li, X. Chen and L. Zhang, *J. Mater. Chem. B*, 2020, **8**, 2627–2635.

122 Y. Huang, X. Ran, Y. Lin, J. Ren and X. Qu, *Chem. Commun.*, 2015, **51**, 4386–4389.

123 C. Zhang, L. Yan, X. Wang, X. Dong, R. Zhou, Z. Gu and Y. Zhao, *Nano Lett.*, 2019, **19**, 1749–1757.

124 Y. Fan, J. Zhang, M. Shi, D. Li, C. Lu, X. Cao, C. Peng, S. Mignani, J. P. Majoral and X. Shi, *Nano Lett.*, 2019, **19**, 1216–1226.



125 Q. Huang, S. Zhang, H. Zhang, Y. Han, H. Liu, F. Ren, Q. Sun, Z. Li and M. Gao, *ACS Nano*, 2019, **13**(2), 1342–1353.

126 C. Lin, Y. Yu, H. G. Zhao, A. Yang, H. Yan and Y. Cui, *Radiother. Oncol.*, 2012, **104**, 395–400.

127 Z. Chen, W. Guo, Q. Wu, L. Tan, T. Ma, C. Fu, J. Yu, X. Ren, J. Wang, P. Liang and X. Meng, *Theranostics*, 2020, **10**, 4659–4675.

128 A. K. Hauser, M. I. Mitov, E. F. Daley, R. C. McGarry, K. W. Anderson and J. Z. Hilt, *Biomaterials*, 2016, **105**, 127–135.

129 C. Yang, X. Mi, H. Su, J. Yang, Y. Gu, L. Zhang, W. Sun, X. Liang and C. Zhang, *Biomater. Sci.*, 2019, **7**, 2076–2090.

130 A. Meidanchi, O. Akhavan, S. Khoei, A. A. Shokri, Z. Hajikarimi and N. Khansari, *Mater. Sci. Eng., C*, 2015, **46**, 394–399.

131 N. G. Shetake, A. Kumar and B. N. Pandey, *Biochim. Biophys. Acta, Gen. Subj.*, 2019, **1863**, 857–869.

132 H. Fakhimikabir, M. B. Tavakoli, A. Zarrabi, A. Amouheidari and S. Rahgozar, *J. Photochem. Photobiol., B*, 2018, **182**, 71–76.

133 S. Jafari, M. Cheki, M. B. Tavakoli, A. Zarrabi, K. Ghazikhhanlu Sani and R. Afzalipour, *J. Biomed. Phys. Eng.*, 2020, **10**, 15–24.

134 Y. H. Gholami, R. Maschmeyer and Z. Kuncic, *Sci. Rep.*, 2019, **9**(1), 1–13.

135 J. Wang, X. Wu, P. Shen, J. Wang, Y. Shen, Y. Shen, T. J. Webster and J. Deng, *Int. J. Nanomed.*, 2020, **15**, 1903–1914.

136 X. Dong, R. Cheng, S. Zhu, H. Liu, R. Zhou, C. Zhang, K. Chen, L. Mei, C. Wang, C. Su, X. Liu, Z. Gu and Y. Zhao, *ACS Nano*, 2020, **14**, 5400–5416.

137 J. Wang, X. Tan, X. Pang, L. Liu, F. Tan and N. Li, *ACS Appl. Mater. Interfaces*, 2016, **8**, 24331–24338.

138 K. Kirakci, J. Zelenka, M. Rumlova, J. Martincik, M. Nikl, T. Ruml and K. Lang, *J. Mater. Chem. B*, 2018, **6**, 4301–4307.

139 K. Kirakci, T. N. Pozmogova, A. Y. Protasevich, G. D. Vavilov, D. V. Stass, M. A. Shestopalov and K. Lang, *Biomater. Sci.*, 2021, **9**, 2893–2902.

140 W. Liu, A. Dong, B. Wang and H. Zhang, *Adv. Sci.*, 2021, **8**, 2003033.

141 L. Chan, X. Chen, P. Gao, J. Xie, Z. Zhang, J. Zhao and T. Chen, *ACS Nano*, 2021, **15**, 3047–3060.

142 H. Huang, L. He, W. Zhou, G. Qu, J. Wang, N. Yang, J. Gao, T. Chen, P. K. Chu and X.-F. Yu, *Biomaterials*, 2018, **171**, 12–22.

143 J. Zhang, Y. Ma, K. Hu, Y. Feng, S. Chen, X. Yang, J. Fong-Chuen Loo, H. Zhang, F. Yin and Z. Li, *Bioconjugate Chem.*, 2019, **30**, 1658–1664.

144 L. Chan, P. Gao, W. Zhou, C. Mei, Y. Huang, X. F. Yu, P. K. Chu and T. Chen, *ACS Nano*, 2018, **12**, 12401–12415.

145 H. Xu, W. Cao and X. Zhang, *Acc. Chem. Res.*, 2013, **46**, 1647–1658.

146 K. E. McColl, M. J. Brodie, R. Whitesmith, K. F. Gray and T. J. Thomson, *Acta Hepatogastroenterol.*, 1979, **26**, 407–412.

147 I. M. Puspitasari, C. Yamazaki, R. Abdulah, M. Putri, S. Kameo, T. Nakano and H. Koyama, *Oncol. Lett.*, 2017, **13**, 449–454.

148 C. Borek, *J. Nutr.*, 2004, **134**, 3207S–3209S.

149 S. O. Evans, P. F. Khairuddin and M. B. Jameson, *Anti-cancer Res.*, 2017, **37**, 6497–6509.

150 D. Schilling, B. Herold, S. E. Combs and T. E. Schmid, *Radiat. Environ. Biophys.*, 2019, **58**, 433–438.

151 E. Handa, I. M. Puspitasari, R. Abdulah, C. Yamazaki, S. Kameo, T. Nakano and H. Koyama, *J. Trace Elem. Med. Biol.*, 2020, **62**, 126653.

152 B. Farhood, K. Mortezaee, E. Motavaseli, H. Mirtavoos-Mahyari, D. Shabeb, A. Elejo Musa, N. S. Sanikhani, M. Najafi and A. Ahmadi, *J. Cell. Biochem.*, 2019, **120**, 18559–18571.

153 L. Y. Cruz, D. Wang and J. Liu, *J. Photochem. Photobiol., B*, 2019, **191**, 123–127.

154 F. Chen, X. H. Zhang, X. D. Hu, P. D. Liu and H. Q. Zhang, *Artif. Cells, Nanomed., Biotechnol.*, 2018, **46**, 937–948.

155 S. Gao, T. Li, Y. Guo, C. Sun, B. Xianyu and H. Xu, *Adv. Mater.*, 2020, **32**, e1907568.

156 U. Shabbir, M. Rubab, E. B. Daliri, R. Chelliah, A. Javed and D. H. Oh, *Nutrients*, 2021, **13**(1), 206.

157 C. Huang, T. Chen, D. Zhu and Q. Huang, *Front. Chem.*, 2020, **8**, 225.

158 T. Ma, Y. Liu, Q. Wu, L. Luo, Y. Cui, X. Wang, X. Chen, L. Tan and X. Meng, *ACS Nano*, 2019, **13**, 4209–4219.

159 J. P. Kelly, T. W. Hannam and G. R. Giles, *Cancer Treat. Rev.*, 1979, **6**(Suppl), 53–61.

160 S. Chen, S. Yu, Z. Du, X. Huang, M. He, S. Long, J. Liu, Y. Lan, D. Yang, H. Wang, S. Li, A. Chen, Y. Hao, Y. Su, C. Wang and S. Luo, *J. Med. Chem.*, 2021, **64**, 3381–3391.

161 H. Liu, Y. Xie, Y. Zhang, Y. Cai, B. Li, H. Mao, Y. Liu, J. Lu, L. Zhang and R. Yu, *Biomaterials*, 2017, **121**, 130–143.

162 S. Masunaga, Y. Uto, H. Nagasawa, H. Hori, K. Nagata, M. Suzuki, Y. Kinashi and K. Ono, *Anticancer Res.*, 2006, **26**, 1261–1270.

163 M. M. Fathy, H. M. Fahmy, O. A. Saad and W. M. Elshemey, *Life Sci.*, 2019, **234**, 116756.

164 S. Shirvalilou, S. Khoei, S. Khoei, S. R. Mahdavi, N. J. Raoufi, M. Motavallian and M. Y. Karimi, *J. Photochem. Photobiol., B*, 2020, **205**, 111827.

165 Y. Xie, Y. Han, X. Zhang, H. Ma, L. Li, R. Yu and H. Liu, *Front. Oncol.*, 2021, **11**, 855.

